RESEARCH ARTICLE | SEPTEMBER 01 2003

# Microscopic theory of linear, entangled polymer chains under rapid deformation including chain stretch and convective constraint release

**Special Collection:** Flow-Induced Crystallization

Richard S. Graham; Alexei E. Likhtman; Tom C. B. McLeish; Scott T. Milner



*J. Rheol.* 47, 1171–1200 (2003)
https://doi.org/10.1122/1.1595099

# Microscopic theory of linear, entangled polymer chains under rapid deformation including chain stretch and convective constraint release

Richard S. Graham,[a] Alexei E. Likhtman, and Tom C. B. McLeish

*Department of Physics and Astronomy, University of Leeds, Leeds LS2 9JT, United Kingdom*

Scott T. Milner

*Kavli Institute for Theoretical Physics, Kohn Hall, University of California at Santa Barbara, Santa Barbara, California 93106*

(Received 3 January 2003; final revision received 19 May 2003)

**Synopsis**

A refined version of the Doi and Edwards tube model for entangled polymer liquids is presented. The model is intended to cover linear chains in the full range of deformation rates from linear to strongly nonlinear flows. The effects of reptation, chain stretch, and convective constraint release are derived from a microscopic stochastic partial differential equation that describes the dynamics of the chain contour down to the length scale of the tube diameter. Contour length fluctuations are also included in an approximate manner. Predictions of mechanical stresses as well as the single chain structure factor under flow are shown. A comparison with experimental data is made in which all model parameters are fixed at universal values or are obtained from linear oscillatory shear measurements. With no parameter modification the model produces good agreement over a wide range of rheological data for entangled polymer solutions, including both nonlinear shear and extension. © *1993 The Society of Rheology.* [DOI: 10.1122/1.1595099]



## I. INTRODUCTION

The tube theory of Doi and Edwards (1986) is remarkably successful in describing a wide range of qualitative features of the rheology of entangled polymer fluids. A recent detailed formulation of the rheological properties of linear polymers, including numerous refinements has produced excellent agreement between theory and experiment in the linear regime [Likhtman and McLeish (2002)]. There have also been attempts to unify the model parameters used for linear polymers with those for chemically identical polymers with different molecular topologies [Pattamaprom *et al.* (2000)]. Despite the ongoing progress a definitive theory for nonlinear flows remains elusive. In particular, it has proven difficult to find consistency in the model parameters used to fit linear and nonlinear data when the assumptions of the Doi–Edwards approach suggest that this ought to be possible. These problems are notoriously manifest in a qualitative failing of the Doi–Edwards (DE) theory in steady state of shear. When steady-state shear stress, $\sigma_{xy}^{SS}$, is plotted as a function of shear rate, $\dot{\gamma}$, the model predicts a shear stress maximum when

[a]Author to whom correspondence should be addressed; electronic mail: rsgraham@umich.edu

the shear rate exceeds the inverse reptation time ($\dot{\gamma} \gtrsim 1/\tau_d$). However, experimental data in this regime indicate that shear stress is a monotonically increasing function of shear rate. Worse still, a consequence of the shear stress maximum is that the DE model predicts a striking shear banding instability occurring in moderately nonlinear flows. Such a feature is not observed in experiments.

Two possible mechanisms to rectify this problem are chain stretch and constraint release. Both processes were discussed by Doi and Edwards but omitted from their constitutive model. Chain stretch refers to configurations in which the length of occupied tube exceeds its equilibrium value. In the DE model chain orientation relaxes on the time-scale of the reptation time, while chain retraction, which is unhindered by tube constraints, occurs at a rate determined by the Rouse time. In entangled systems these two times scales are reasonably well separated, $\tau_d/\tau_R = 3Z$ where $Z$ is the number of chain entanglements. Consequently, it is, in principle, possible to model moderately nonlinear flows, in which $\dot{\gamma}\tau_d \gtrsim 1$ and $\dot{\gamma}\tau_R \ll 1$, by assuming retraction occurs instantaneously. However, the effect of chain stretch becomes significant when $\dot{\gamma}\tau_R \gtrsim 1$, a regime which is accessible in well controlled experiments on entangled polymers, particularly in shear. A refinement to the DE model known as the Doi–Edwards–Marrucci–Grizzuti (DEMG) theory [Marrucci and Grizzuti (1988); Pearson *et al.* (1991); Mead and Leal (1995)] adds stretch to the basic DE model. The inclusion of stretch improves transient predictions in startup of shear in several ways. The DEMG model predicts transient overshoots in shear stress and normal stress that grow in size with shear rate. In addition, the strain at peak stress of these overshoots grows with shear rate. All of these features are observed experimentally. The DEMG theory is less successful in steady state of shear. In many circumstances the theory still predicts a shear stress maximum. In fact, any approach that merely adds chain stretch, relaxing via Rouse retraction, to the DE theory is doomed to suffer a similar fate. The reasons for this are twofold. In rapid shear flows the DE orientation tensor predicts strong steady-state chain alignment along the shear direction. As a consequence, the highly aligned chains present a very slim profile to the velocity gradient and so predicted steady-state stretch values are modest even at high stretch Weissenberg numbers ($W_s = \dot{\gamma}\tau_R$). A more fundamental problem is that the separation of orientation time, $\tau_d$, and stretch time, $\tau_R$, is fixed at $3Z$. Hence, if $Z$ is set to a large enough value the onset of chain stretch is delayed to shear rates well in excess of $1/\tau_d$ and the bare DE behavior, including the stress maximum, is recovered at shear rates around $1/\tau_d$. The degree of entanglement necessary to see this effect is within the range of existing experiments.

A second possible solution is constraint release. This is an additional relaxation mechanism that recognises that whenever a chain end passes through a tube segment the constraint that was imposed by this chain on a neighboring chain is lost. Hence, the neighboring chain is free to explore a wider region via lateral motion (see Fig. 1). Constraint release is a self consistent closure of the mean field approximation of the tube model. In the linear regime constraint release events are caused by reptation of the surrounding chains. This is known as reptative or thermal constraint release. Since reptative constraint release occurs on the time-scale of the reptation time of the whole chain and one event only relaxes a small part of the chain Doi and Edwards argued that has a negligible effect on relaxation. However, Likhtman and McLeish (2002) demonstrated that constraint release has significant effects near the terminal time. In addition, constraint release becomes increasingly important in the nonlinear regime. In a crucial insight, Marrucci (1996) demonstrated that in nonlinear flows, chain retraction also contributes to the constraint release rate. The effect of chain retraction greatly increases the influence of

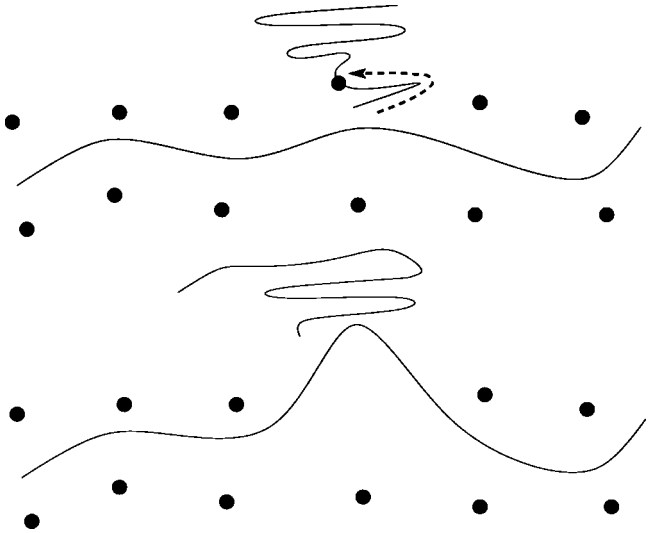

**FIG. 1.** Schematic representation of a constraint release event.

constraint release. The release rate grows with the convection rate, becoming of order of the shear rate at high rates. This process is known as convective constraint release (CCR) since tube constraints are swept away by the convection. The mechanism becomes significant as $\dot{\gamma}$ approaches $1/\tau_d$, precisely the rate as which the Doi Edwards model begins to fail.

There have been various attempts to incorporate CCR into a constitutive model both without chain stretch [Ianniruberto and Marrucci (1996); Ianniruberto and Marrucci (2000)] and more recently with stretch [Ianniruberto and Marrucci (2001); Mead *et al.* (1998)]. However, all of these theories model the effect of CCR by directly modifying the overall chain relaxation time. Effectively, the relaxation time becomes dependent on the molecular response to the deformation. While the arguments for this modification are molecularly motivated, the connection between constraint release and the global relaxation time is, in the end, heuristic. Additionally, the assumption that CCR acts in a global manner destroys any molecular detail on length scales of less than the overall chain length. Thus, only rudimentary predictions for quantities that are sensitive to finer molecular structure such as the single chain structure factor can be made. New experimental techniques, in addition to mechanical stress measurements, are proving to be useful tests of molecular based theories [McLeish *et al.* (1999); McLeish (2002); Wischnewski *et al.* (2002); Müller *et al.* (1993); Watanabe *et al.* (2002)]. A consideration of the local influence of constraint release is essential in this context. The idea of the tube itself experiencing constraint release being modeled as a Rouse object was postulated by de Gennes (1975). It utilizes the fact that the Rouse model generically describes the global behavior of the local jump model for a connected object. The approach allows a description of constraint release down to the length-scale of the tube diameter. Viovy *et al.* (1991) formulated these ideas to model the linear rheology of bimodal blends. With a careful choice of blend composition Rouse tube motion can be directly observed in experimental data in the linear regime [Rubinstein and Colby (1988)]. Recently Milner *et al.* (2001) and Likhtman *et al.* (2000) derived a nonlinear constitutive model by treating CCR as local Rouse-like tube motion. Their model is intended to cover only nonstretching flows in order to consider the CCR mechanism in isolation. The approach successfully elimi-

nates the shear stress maximum without relying on chain stretch. In addition, since the model is able to make detailed predictions for the single chain structure factor, it offers an explanation for the relatively low anisotropy observed in sheared melts [Müller *et al.* (1993)] when compared to the predictions of the DE theory. However, in practice it is very hard to remove the effects of chain stretch as in the best characterized experiments, the degree of entanglement is never extreme. The inclusion of chain stretch into a Rouse-tube theory of entangled dynamics is therefore urgent. In this paper we propose a generalization of the Milner *et al.* (2001) theory in which the chain retraction is not instantaneous. We review the Milner McLeish and Likhtman model in Sec. II and generalize the model to cover stretching flows in Sec. III. An approximate treatment of contour length fluctuations (CLF) is added in Sec. IV. The inclusion of contour length fluctuations is not a luxury—it enables a proper quantitative comparison with experimental data and a correct limit in linear response. A numerical method of solution is outlined in Sec. V and we present the model predictions in Sec. VI, focusing on the difficulties discussed above. Finally, we compare the theory with published experimental data on nearly monodisperse entangled solutions of linear polymers under shear and extension in Sec. VII.

## II. MILNER, MCLEISH, AND LIKHTMAN MODEL

In this section we present a brief review of the model of Milner, McLeish, and Likhtman (2001) (MML) for convective constraint release. The model describes the dynamics of a monodisperse melt of entangled, linear polymer molecules under a strong deformation. The chain is confined to a tube of diameter $a$ due to constraints formed by surrounding chains and the aim of the model is to derive dynamic equations for the entire configuration of a single chain down to the length-scale of the tube diameter. The configuration is described by the space curve $\mathbf{R}(s,t)$, which denotes the position vector of tube segment $s$ at time $t$. The tube comprises of $Z = M/M_e$ segments and $s$ spans the chain length, running from 0 to Z. From a knowledge of the chain shape various macroscopic quantities can be deduced.

The model accounts for a range of sources of motion and each process has a corresponding term in the stochastic partial differential equation that models the dynamics of the entire chain. The simplest of these is convection due to the applied deformation. The deformation is described by the velocity gradient tensor $\boldsymbol{\kappa} = \boldsymbol{\nabla}\mathbf{v}$ and all points on the chain move affinely with the flow. Relaxation is then relative to this affine motion. Three relaxation mechanisms act on each tube segment. The first of these is reptation which is curvilinear diffusion of the entire chain along its own contour. This processes relaxes stress since the chain ends escaping the tube are free to choose any new orientation. The expression for reptation is taken directly from the original DE model. The second process is CCR, which is assumed to act at an equal rate at all points along the chain. It is modeled by Rouse tube hops of length $a$ and frequency $\nu$. Finally, retraction acts along the tube contour, holding the total length fixed at its equilibrium value. The retraction rate is proportional to the distance of the segment from the chain center and the constant of proportionality, $\lambda$, is chosen at each instant to maintain the chain at its equilibrium length. Figure 2 shows these processes schematically. Collecting all terms together into a stochastic difference equation for a single chain gives

$$\mathbf{R}(s,t+\Delta t) = \mathbf{R}(s+\Delta\xi(t),t)+\Delta t\left(\boldsymbol{\kappa}\cdot\mathbf{R}+\frac{3\nu}{2}\frac{\partial^2\mathbf{R}}{\partial s^2}+\mathbf{g}(s,t)+\lambda\left(\frac{Z}{2}-s\right)\frac{\partial\mathbf{R}}{\partial s}\right). \quad (1)$$

The terms in Eq. (1) represent reptation, convection, CCR and retraction, respectively. Equation (1) contains two noise terms: $\Delta\xi(t)$ describes the displacement of the chain due

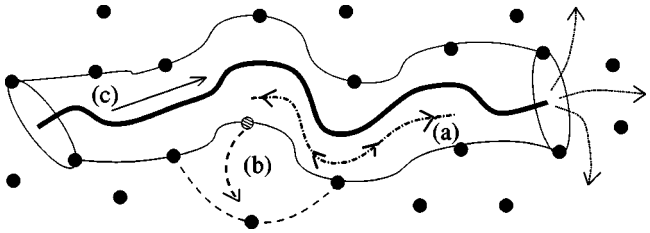


**FIG. 2.** Three relaxation mechanism available to an unbranched, entangled polymer chain: (a) reptation, (b) constraint release, and (c) retraction.

to Brownian diffusion along the tube (reptation) and $\mathbf{g}(s,t)$ describes motion due to random constraint release events. Both terms are mean zero Gaussian and have the following second moments:

$$\begin{aligned} \langle \Delta\xi(t)\Delta\xi(t')\rangle &= \frac{2}{3\pi^2 Z\tau_e}\delta(t-t'), \\ \langle g_\alpha(s,t)g_\beta(s',t')\rangle &= \nu a^2\delta(s-s')\delta(t-t')\delta_{\alpha\beta}. \end{aligned} \tag{2}$$

The angular brackets denote averages over an ensemble of chains and the indices $\alpha$ and $\beta$ denote Cartesian components. The local time scale for the model is set by $\tau_e$ which is the Rouse time of a single entanglement segment. This leaves the constraint release rate, $\nu$, as the only remaining unknown quantity. It can be determined self-consistently from the retraction rate, $\lambda$, via the equation

$$\nu = c_\nu\left(\lambda + \frac{4}{\pi^2 Z^3\tau_e}\right). \tag{3}$$

Equation (3) counts the constraint release from retraction and the preaveraged contribution from reptation, respectively, with the parameter $c_\nu$ determining the number of retraction events necessary to result in one tube hop of a tube diameter. Milner *et al.* (2001) argue that entanglements result from ''the mutual, delocalized topological interaction of many structures'' and so several retraction events are required to produce a tube hop of length $a$. Consequently, a value of $c_\nu \leqslant 1$ is expected.

The stress and single chain structure factor both follow from a knowledge of the chain configuration, $\mathbf{R}(s,t)$. The stress tensor, $\boldsymbol{\sigma}$, is given by

$$\sigma_{\alpha\beta} = \frac{c}{N}\frac{3k_BT}{a^2}\int_0^Z\left\langle\frac{\partial R_\alpha(s)}{\partial s}\frac{\partial R_\beta(s)}{\partial s}\right\rangle ds. \tag{4}$$

Here, $c/N$ is the polymer chain concentration. The single chain structure factor is obtained from

$$S(\mathbf{q}) = \int_0^Z\int_0^Z \exp\left(-\sum_{\alpha,\beta}\frac{q_\alpha q_\beta}{2}\int_s^{s'}\int_s^{s'}\left\langle\frac{\partial R_\alpha(s_1)}{\partial s}\frac{\partial R_\beta(s_2)}{\partial s'}\right\rangle ds_1 ds_2\right) ds ds'. \tag{5}$$

Equations 4 and 5 show that a knowledge of the function

$$f_{\alpha\beta}(s,s') = \left\langle\frac{\partial R_\alpha(s)}{\partial s}\frac{\partial R_\beta(s')}{\partial s'}\right\rangle$$

is sufficient to evaluate both the stress and the single chain structure factor. By taking suitable averages of Eq. (1) a deterministic partial differential equation (PDE) for $\mathbf{f}(s,s')$ can be obtained. In deriving an expression for $f_{\alpha\beta}(s,s')$ the following closure approximation is necessary.

$$\langle R_\alpha(s,t)R_\beta(s',t)\lambda(t)\rangle \approx \lambda(t)\langle R_\alpha(s,t)R_\beta(s',t)\rangle. \tag{6}$$

Milner *et al.* (2001) verified this approximation by direct stochastic simulation of equation 1 and found it to be valid whenever CCR is the dominant relaxation mechanism, namely whenever $1/\tau_d \ll \dot{\gamma} \ll 1/\tau_R$. The resulting PDE for $\mathbf{f}(s,s')$ is then solved by converting to a Fourier sine series.

## III. TUBE MODEL FOR LINEAR POLYMERS WITH CCR AND STRETCH

Steady-state shear stress measurements on nearly monodisperse entangled polymer liquids typically show three regimes of behavior with increasing shear rate [Bercea *et al.* (1993); Menezes and Graessley (1982); Menezes (1980)]. At low shear rates ($\dot{\gamma}\tau_d < 1$) the stress increases linearly with shear rate, at intermediate rates ($1/\tau_d < \dot{\gamma} < 1/\tau_R$) there is a region of nearly constant shear stress and at high rates ($\dot{\gamma}\tau_R > 1$) the stress shows a steeper gradient. Thus, the overall steady flow curve is a monotonically increasing function of shear rate. The MML theory accounts for the first two of these regimes. Reptation is the dominant relaxation in the linear regime and CCR controls the plateau region. The third regime has been widely attributed to the influence of chain stretch. We aim to generalize the MML theory to cover stretching flows, thus extending its region of validity in the steady flow curve and testing our understanding of transient shear flows. The approach of our generalisation is to introduce any new physics necessary to model stretching flows directly into Eq. (1), produce a deterministic PDE for the tube tangent correlation function by taking suitable averages and to solve this equation using an appropriate numerical scheme.

### A. Rouse retraction term

To model the effect of finite rate retraction we replace the instantaneous retraction term in equation 1 with a term that arises from Rouse motion of the chain inside its tube. The force-extension law for the chain is the usual linear spring relationship. Hence a microscopic force balance for this term at tube segment $s$ gives $N_e\zeta_0(\partial\mathbf{R}/\partial t) = (3k_BT/N_eb^2)\mathbf{R}''(s)$ where the primes denote derivatives with respect to $s$, $\zeta_0$ is the monomer friction constant and $b$ is the Kuhn step length. Retraction acts only along the tube direction so we project the retraction force along the unit tangent vector to the tube $\mathbf{R}'(s)/|\mathbf{R}'(s)|$. By introducing $\tau_e = (\zeta_0 b^2 N_e^2/3\pi^2 k_BT)$ the new retraction terms reads

$$\frac{\partial\mathbf{R}(s)}{\partial t} = \cdots + \frac{1}{\pi^2\tau_e}\frac{(\mathbf{R}''(s)\cdot\mathbf{R}'(s))}{|\mathbf{R}'(s)|^2}\mathbf{R}'(s)$$

$$= \cdots + \frac{1}{2\pi^2\tau_e}\left(\frac{\partial}{\partial s}\ln[\mathbf{R}'(s)\cdot\mathbf{R}'(s)]\right)\mathbf{R}'(s). \tag{7}$$

This term necessitates a stricter application of the boundary conditions at the chain ends than in the approach of Milner *et al.* (2001). The end tangent vectors should be isotropic vectors of length $a$ at all times so ensuring a totally relaxed condition for both orientation and stretch at all times. The length condition fixes the tube equilibrium length to its correct value and the isotropic condition ensures that as a chain end escapes the tube it takes on a random orientation. These boundary conditions are not straightforward to express in terms of $\mathbf{R}$ and are more readily expressed for the tangent vector correlation

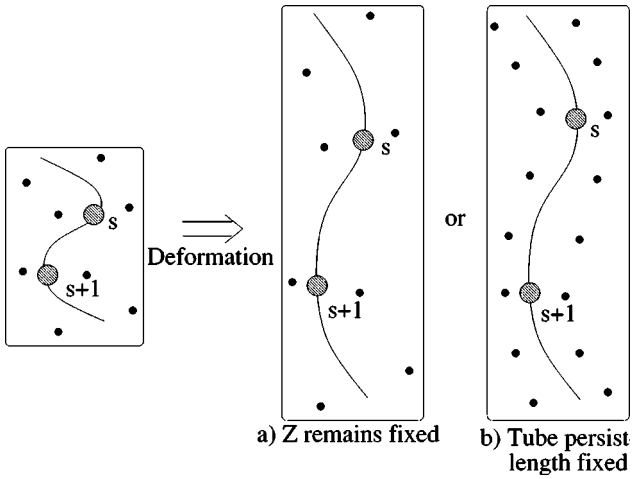


**FIG. 3.** Two possibilities for the effect of a step deformation on the entanglement network. (a) Number of entanglements points is fixed, and so the tube persistence length grows. (b) Tube persistence length remains fixed, so $Z$ grows in proportion with the primitive path length.

function, $\mathbf{f}(s,s') = \langle \mathbf{R}'(s)\mathbf{R}'(s')\rangle$, and so further discussion of the boundary conditions is delayed until a full formulation in terms of $\mathbf{f}(s,s')$ is introduced.

### B. Tube diameter and persistence length under deformation

The retraction term in Eq. (7) allows the accumulation of chain stretch in a sufficiently rapid deformation. Consequently, further modifications of equation 1 are needed to model the influence of chain stretch on the other relaxation processes. Before these modifications can be made the question summarized in Fig. 3 must be answered. Under the influence of a strong deformation how does the entanglement network deform with the test chain? We note that it is possible that both the tube diameter and tube persistence length change under deformation. If we assume a constant tube diameter the two simplest possibilities are that the number of entanglements experienced by the chain remains at its equilibrium value and, effectively, the tube persistence length grows (a) or the number of entanglements increases in proportion with the primitive path length of the chain (b). This corresponds to a tube persistence length which is fixed under deformation. The arguments for scenario (b), the constant tube persistence length, appear to be stronger for a variety of reasons. Our theory is explicitly applicable only to volume conserving deformations, hence, the monomer density surrounding the test chain is not strain dependent. While the theory covers rapid deformations these deformations are still slow with respect to the local relaxation time on the scale of the tube diameter, $\tau_e$. Since entanglements should be considered as mutual, delocalized topological interactions acting on a length scale of the tube diameter, the melt structure on this scale is not strongly perturbed from that of an equilibrium melt. We will assume scenario (b) from now on, but will be mindful that this choice directly affects how the local chain stretch influences the other relaxation mechanisms. It should be noted that other scenarios are plausible, including nonaffine changes to the tube diameter. For such effects in networks see Rubinstein and Panyukov (1997).

As a direct consequence of choosing a fixed tube persistence length the CCR term in Eq. (1) has to be modified. The physical reason for this modification is shown in Fig. 3. For an unstretched chain (a) the number of tube segments between bead $s$ and bead $s+1$ is one. However, for a stretched chain (b) the number of segments is increased. The

value is now proportional to the local stretch ratio ($|\mathbf{R}'(s)|/a$). Therefore, $(|\mathbf{R}'(s)|/a)^2$ times as many tube hops are necessary to relax the chain segment between $s$ and $s+1$. However, the spring constant of each entanglement segment is increased by a factor of the local stretch. The net result is that the local influence of CCR is reduced by a single factor of $|\mathbf{R}'(s)|/a$. A more detailed derivation based on this argument is given in Appendix A. The renormalized CCR term is

$$\frac{\partial \mathbf{R}(s)}{\partial t} = \cdots + \frac{3\nu}{2}\frac{a}{|\mathbf{R}'(s)|}\mathbf{R}''(s) + \tilde{\mathbf{g}}(s,t). \tag{8}$$

Similarly, the corresponding noise term is also renormalized because of the greater number of constraint release sites per local contour, in proportion with the local stretch ratio.

$$\langle \tilde{g}_\alpha(s,t)\tilde{g}_\beta(s',t)\rangle = \nu a^2 \frac{a}{|\langle \mathbf{R}'(s)\rangle|}\Delta(s-s')\delta_{\alpha\beta}. \tag{9}$$

We note that these two renormalisations are consistent with the fluctuation–dissipation theorem, which itself applies to the CCR Rouse relaxation system, even though it is not thermal, because it does drive the melt towards equilibrium. It is important to remember that although we are using a continuous description, the model only describes the chain correlation function on length scales greater than the tube diameter, $a$. The function $\Delta(s-s')$ is not infinitely high and thin, as in Milner *et al.* (2001), where a true delta function was used, but it persists over a tube diameter with a height of one. Thus, we use the form

$$\Delta(s-s') = \begin{cases} 1 & \text{for } |s-s'| < \dfrac{1}{2}. \\ 0 & \text{otherwise} \end{cases} \tag{10}$$

This distinction is necessary since the solutions of the model are sensitive to the short length scale cut off of this function and so this cut off must explicitly be the tube diameter.

### C. CCR stretch relaxation

Chain stretch can also be relaxed by CCR. This was demonstrated by Mead *et al.* (1998) who discussed this at length. The mechanism is summarized in Fig. 4. The choice of Rouse tube hops is influenced by the local stretch since tube hops that relax local stretch will become increasingly energetically favorable as the chain stretch increases. Hence, the distribution of CCR events between relaxing chain stretch and chain orientation depends upon the local chain stretch. Mead *et al.* (1998) introduced an *ad hoc* function of chain stretch to switch the relaxation of CCR between orientation and stretch. An advantage of our more detailed local consideration of CCR is that the Rouse tube hopping term in Eq. (1) is already weighted by the local potential due to chain stretch. This term already contains the above mechanism in the balance between the terms $(3\nu/2)\,\mathbf{R}''(s)$ and $\mathbf{g}(s)$. No ''switch function'' is necessary since both stretch and orientation are implicitly contained in the solution of $\mathbf{f}(s,s')$ as a result of employing a local model of CCR from the outset.

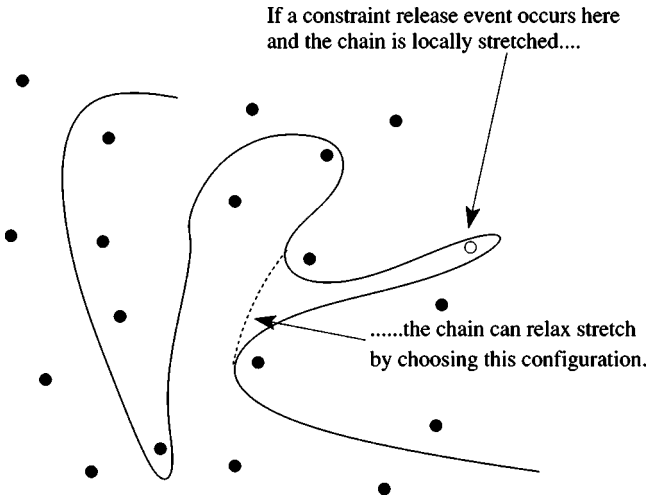


**FIG. 4.** Mechanism by which CCR relaxes chain stretch.

### D. Suppression of reptation due to stretch

The term $\mathbf{R}(s,t+\Delta t) = \mathbf{R}[s+\Delta\xi(t),t]$ in Eq. (1) models reptation by stating that in a time interval $\Delta t$ the monomer that was at position $s$ at time $t$ shifts to the position that was previously occupied by monomer $s+\Delta\xi(t)$. This argument is only valid if the monomers are at their equilibrium separation. For a stretched chain the above term artificially accelerates reptation in proportion with the chain length since the physical distance that a monomer must diffuse to relax is longer in a stretched chain. To ensure that the chain diffusion occurs at a constant rate in real space rather than monomer space we reduce the displacement due to reptation by a factor of $Z/Z^*(t)$, where $Z^*(t)$ is the number of tube segments occupied by the stretched chain. The new reptation term is

$$\mathbf{R}(s,t+\Delta t) = \mathbf{R}\left(s+\frac{Z}{Z^*(t)}\Delta\xi(t),t\right). \tag{11}$$

The effective number of entanglements is proportional to the arc length of the primitive path and Eq. (20) gives an expression for $Z^*(t)$. It might be argued that Eq. (11) suppresses reptation with a global expression for the chain stretch whereas it would be more accurate to use the local value of the chain stretch at each point along the chain, $[a/\mathbf{R}'(s)]$. This more detailed procedure was checked and the results were not sensitive to this alteration and so we use Eq. (11) for simplicity.

### E. Microscopic equation of motion

Collecting together the modified expressions for reptation, CCR and retraction [Eqs. (7), (8), and (11)], expanding the reptation term to second order in $\Delta\xi(t)$, we obtain the following microscopic stochastic difference equation, which replaces Eq. (1):

$$\mathbf{R}(s,t+\Delta t) = \mathbf{R}(s,t)+\Delta\xi(t)\frac{Z}{Z^*(t)}\frac{\partial\mathbf{R}}{\partial s}+\frac{\Delta\xi(t)^2}{2}\frac{Z^2}{Z^*(t)^2}\frac{\partial^2\mathbf{R}}{\partial s^2} + \Delta t\left[\boldsymbol{\kappa}\cdot\mathbf{R}+\frac{3\nu}{2}\frac{a}{|\mathbf{R}'(s)|}\mathbf{R}''(s)+\tilde{g}(s,t)+\frac{1}{2\pi^2\tau_e}\left(\mathbf{R}'\frac{\partial}{\partial s}\ln(\mathbf{R}'\cdot\mathbf{R}')\right)\right]. \tag{12}$$

The second and third terms on the right-hand side describe reptation, the fourth is the effect of convection, the fifth and sixth correspond to the action of constraint release, and the final term accounts for chain retraction. The local time scale of the model is fixed by $\tau_e$, the Rouse time of an entanglement segment. A knowledge of $\tau_e$ and the number of entanglements, $Z$, is sufficient to define the reptation time, $\tau_d$, and the chain Rouse time, $\tau_R$:

$$\tau_d = 3Z^3\tau_e, \quad \tau_R = Z^2\tau_e. \tag{13}$$

Neither of these time scales is explicitly fed into the model but they are the natural characteristic time scales of the solutions of Eq. (12).

### F. Equation for the tangent correlation function

Following the approach of Milner *et al.* (2001) a time evolution equation for $\mathbf{f}(s,s') = \langle\mathbf{R}'(s)\mathbf{R}'(s')\rangle$ can be found from Eq. (12):

$$\frac{\partial f_{\alpha\beta}(s,s')}{\partial t} = \frac{\partial^2}{\partial s\partial s'}\left(\lim_{\Delta t\to 0}\frac{\langle R_\alpha(s,t+\Delta t)R_\beta(s',t+\Delta t)\rangle-\langle R_\alpha(s,t)R_\beta(s',t)\rangle}{\Delta t}\right). \tag{14}$$

An expression for the term $\langle R_\alpha(s,t+\Delta t)R_\beta(s',t+\Delta t)\rangle$ is found by taking suitable averages of Eq. (12) using the known moments of the two noise terms, the fact that the reptative noise is not correlated with the chain configuration and the Ito–Stratonovich relation:

$$\langle\tilde{g}_\alpha(s,t)R_\beta(s',t)\rangle = \frac{1}{2}\nu a^2\frac{a}{\langle|\mathbf{R}'(s)|\rangle}\Delta(s-s')\,\delta_{\alpha\beta}. \tag{15}$$

In order to obtain a closed expression for $\mathbf{f}(s,s')$, the following closure approximations are necessary. In the retraction term, we approximate

$$\left\langle R'_\alpha(s)R_\beta(s')\frac{\partial}{\partial s}\ln[\mathbf{R}'(s)\cdot\mathbf{R}'(s)]\right\rangle \approx \mathcal{R}_s\langle R'_\alpha(s)R_\beta(s')\rangle\frac{\partial}{\partial s}\ln[\langle\mathbf{R}'(s)\cdot\mathbf{R}'(s)\rangle], \tag{16}$$

where $\mathcal{R}_s$ is, to a first approximation, an order unity geometric prefactor that optimizes the decoupling approximation. For narrow distributions of $\mathbf{R}'(s)$, we would anticipate $\mathcal{R}_s = 1$, but for broad distributions around a zero mean, rounding permutations of possible decouplings suggests $\mathcal{R}_s > 1$. For a discussion of the optimal value see Sec. VII C. In the CCR term we use

$$\left\langle\frac{R''_\alpha(s)R_\beta(s')}{|\mathbf{R}'(s)|}\right\rangle \approx \frac{\langle R''_\alpha(s)R_\beta(s')\rangle}{\sqrt{\langle|\mathbf{R}'(s)|^2\rangle}}. \tag{17}$$

This leads to a PDE for $\mathbf{f}(s,s')$, which is suitable for direct solution,

$$\frac{\partial \mathbf{f}}{\partial t} = \boldsymbol{\kappa}\cdot\mathbf{f}+\mathbf{f}\cdot\boldsymbol{\kappa}^T+\frac{1}{3\pi^2 Z\tau_e}\left(\frac{Z}{Z^*(t)}\right)^2\left(\frac{\partial}{\partial s}+\frac{\partial}{\partial s'}\right)^2\mathbf{f}$$
$$+\frac{3\nu a}{2}\left[\frac{\partial}{\partial s}\left(\frac{a}{\sqrt{\mathrm{Tr}\,\mathbf{f}(s,s)}}\frac{\partial}{\partial s}(\mathbf{f}-\mathbf{f}^{\mathrm{eq}})\right)+\frac{\partial}{\partial s'}\left(\frac{a}{\sqrt{\mathrm{Tr}\,\mathbf{f}(s',s')}}\frac{\partial}{\partial s'}(\mathbf{f}-\mathbf{f}^{\mathrm{eq}})\right)\right]$$
$$+\frac{\mathcal{R}_s}{2\pi^2\tau_e}\left[\frac{\partial}{\partial s}\left(\mathbf{f}\frac{\partial}{\partial s}\ln[\mathrm{Tr}\,\mathbf{f}(s,s)]\right)+\frac{\partial}{\partial s'}\left(\mathbf{f}\frac{\partial}{\partial s'}\ln[\mathrm{Tr}\,\mathbf{f}(s',s')]\right)\right]. \tag{18}$$

We also use the identity $\partial/\partial s\,\mathbf{f}^{\mathrm{eq}} = -\partial/\partial s'\,\mathbf{f}^{\mathrm{eq}}$ in deriving Eq. (18). The spatial arguments of $\mathbf{f}$ are $(s,s')$ unless shown otherwise. The equilibrium value of $\mathbf{f}$ is determined by the CCR noise term and is given by

$$\mathbf{f}^{\mathrm{eq}} = \frac{a^2}{3}\Delta(s-s')\mathbf{I}. \tag{19}$$

As discussed above, the boundary conditions are more easily expressed in terms of $\mathbf{f}$ than $\mathbf{R}$ and so can be introduced at this stage. The conditions must be applied on the perimeter of the square region given by $s,s' = 0$–$Z$. The correlation $\mathbf{f}(s,s')$ is zero everywhere on the perimeter except at the two diagonally opposite corners, $s,s' = 0$ and $s,s' = Z$, where $\mathbf{f} = a^2\mathbf{I}/3$. Essentially, the two end vectors must be isotropic, uncorrelated with any other point on the chain and of length $a$. The configuration of $\mathbf{f}^{\mathrm{eq}}$ describes a chain distribution for which this is true at every point along the chain. Hence, $\mathbf{f}^{\mathrm{eq}}$ obeys the given boundary conditions.

Equation (18), along with boundary conditions, describes the dynamics of the tube tangent correlation function, $\mathbf{f}(s,s')$. However, it requires expressions for the instantaneous number of entanglements, $Z^*(t)$, and the constraint release rate, $\nu$, both of which depend on the instantaneous chain configuration. In the following sections we derive expressions for these quantities in terms of $\mathbf{f}(s,s')$.

### G. Number of entanglements

Since the tube diameter is assumed to be fixed the chain accumulates additional entanglements as it stretches. The instantaneous number of entanglements, $Z^*(t)$, is the normalized arc length of the primitive path,

$$Z^*(t) = \int_0^Z \sqrt{\langle \mathbf{R}'(s)\cdot\mathbf{R}'(s)/a^2\rangle}\,ds = \frac{1}{a}\int_0^Z \sqrt{\mathrm{Tr}\,\mathbf{f}(s,s)}\,ds, \tag{20}$$

where we have assumed that

$$\langle\sqrt{\mathbf{R}'(s)\cdot\mathbf{R}'(s)}\rangle \approx \sqrt{\langle\mathbf{R}'(s)\cdot\mathbf{R}'(s)\rangle}.$$

### H. Constraint release rate

We require an expression for the constraint release rate due to retraction, $\lambda$, which must be found self consistently from the current chain configuration. Physically, the retraction rate is the frequency with which one chain end retracts a distance of the tube

diameter. The frequency of constraint release events per chain is rate of change of length of the chain due to retraction divided by $a$. The rate per constraint, $\lambda$, is $1/Z^*(t)$ times this value,

$$\lambda = -\frac{1}{Z^*(t)}\frac{\partial}{\partial t}\int_0^Z \frac{1}{a}\sqrt{\mathrm{Tr}\,\mathbf{f}(s,s)}\big|_{\mathrm{retraction}} ds$$

$$= -\frac{\mathcal{R}_s}{2aZ^*(t)\pi^2\tau_e}\int_0^Z \frac{1}{\sqrt{\mathrm{Tr}\,\mathbf{f}(s,s)}}\frac{\partial}{\partial s}\left(\mathrm{Tr}\,\mathbf{f}(s,s')\frac{\partial}{\partial s}\ln[\mathrm{Tr}\,\mathbf{f}(s,s)]\right)\Bigg|_{s'=s} ds, \tag{21}$$

where the rate of change of $\mathrm{Tr}\,\mathbf{f}(s,s)$ due to retraction is found using just the retraction term from Eq. (18). Finally, the total constraint release rate, $\nu$, can be found from

$$\nu = c_\nu\left(\lambda + \frac{4}{\pi^2 Z^2 Z^*(t)\tau_e}\right). \tag{22}$$

## IV. CONTOUR LENGTH FLUCTUATIONS

In real polymers the primitive chain path length continually fluctuates about its mean value due to thermal noise. This process allows $\sim\sqrt{Z}$ tube segments at each end to relax faster than by reptation. Thus, if the number of entanglements is relatively small, as is usually the case with real polymers, contour length fluctuations can relax a significant proportion of the chain far faster than reptation. CLF can, in principle, be accounted for by replacing the reptation noise term, $\Delta\xi(t)$, with a term in which each point on the chain contour has an independent thermal force. However, a rigorous solution of this system for a general nonlinear flow is a formidable problem. A more tractable approach is to embed an account of CLF within our formulation, guided by more detailed theories of linear rheology. In this work we incorporate CLF in an approximate way that is consistent with the linear theory of Likhtman and McLeish (2002) in the limit of small deformation rates. We account for the rapid relaxation of the chain ends by replacing the fixed diffusion constant in the reptation term of Eq. (18) by a function, $D_{\mathrm{CLF}}(s,s')$, which depends upon position along the chain contour. We choose a form for $D_{\mathrm{CLF}}(s,s')$ by drawing upon the more rigorous linear treatments of CLF by Likhtman and McLeish (2002). This suggests that close to the chain end the relaxation rate should vary as $s^{-2}$ to produce the correct early time behavior, $\sigma(t) \sim 1 - ct^{1/4}$, and that far from the chain ends CLF should be suppressed, making reptation the dominant mechanism. From this argument we obtain the following form of an effective one-dimensional diffusion constant, which covers the relaxation of local correlations ($s = s'$) of the tangent correlation function.

$$D_{1d}(s) = \begin{cases} \dfrac{\alpha_d^2}{s^2} & s < \alpha_d\sqrt{Z} \\ \dfrac{\alpha_d^2}{(Z-s)^2} & Z-s < \alpha_d\sqrt{Z} \\ 1/Z & \text{otherwise} \end{cases}. \tag{23}$$

However, our formalism requires a two-dimensional function, $D_{\mathrm{CLF}}(s,s')$, that describes the relaxation of tangent correlations of two separate points on the chain. We obtain this

function by assuming that, due to the strong dependence of relaxation rate on contour position, the relaxation rate of two separate points on the chain is dominated by the relaxation of the faster of the points. This leads to

$$D_{\mathrm{CLF}}(s,s') = D_{1d}(s_{\min}), \tag{24}$$

where $s_{\min} = \mathrm{Min}(s,s',Z-s,Z-s')$. Using this approach it is also possible to include the suppression of CLF by the local stretch through a similar argument to Sec. III D. (see Appendix B for a derivation of this term). The new term in the **f** equation is finally

$$\frac{\partial \mathbf{f}}{\partial t} = \cdots + \frac{1}{3\pi^2\tau_e}\frac{a}{\sqrt{\mathrm{Tr}\,\mathbf{f}(s_{\min},s_{\min})}}\left(\frac{\partial}{\partial s}+\frac{\partial}{\partial s'}\right)\left[\frac{aD_{\mathrm{CLF}}(s,s')}{\sqrt{\mathrm{Tr}\,\mathbf{f}(s_{\min},s_{\min})}}\left(\frac{\partial}{\partial s}+\frac{\partial}{\partial s'}\right)\mathbf{f}\right]. \tag{25}$$

We fix the constant $\alpha_d$ by insisting that the predictions of the model for the complex modulus, $G'(\omega)$ and $G''(\omega)$, under linear oscillatory shear should agree with the exact treatment of Likhtman and McLeish (2002). The comparison was performed with constraint release removed ($c_\nu = 0$) and values of $Z$ ranging from 6 to 40. Choosing $\alpha_d = 1.15$ was found to provide agreement to within typical experimental error between the two theories for frequencies up to $\omega\tau_e \sim 1$ for all of the tested values of $Z$, indicating that the chosen implementation of CLF accurately approximates the first passage time of a Rouse chain in a tube. The small moderation of the linear spectrum in the range $\tau_R^{-1} < \omega < \tau_e^{-1}$ arising from longitudinal Rouse modes [Likhtman and McLeish (2002)] is also accounted for by this parametrization.

### A. Thermal constraint release from contour length fluctuations

The additional mobility of the chain end due to CLF, above that from reptation, must also be accounted for in the constraint release rate. For moderately entangled materials, constraint release from CLF can be significant in a linear flow. We account for this by adjusting the reptative constraint release term in Eq. (3). In reality, the chain experiences a broad spectrum of constraint release (CR) rates due to both reptation and CLF, however, we approximate this process with a single linear constraint release rate. This produces a weak dependence of the prefactor in the term for reptation constraint release (rcr) on both $Z$ and $c_\nu$. In contrast, a full theory for CR faithful to the whole spectrum of CR, such as Likhtman and McLeish (2002), would not require such a prefactor. Thus,

$$\nu = c_\nu\left(\lambda + \frac{1}{3\beta_{\mathrm{rcr}}(Z,c_\nu)Z^2\tau_e}\right). \tag{26}$$

We fix $\beta_{\mathrm{rcr}}(Z)$ by taking a power series in $1/\sqrt{Z}$, the appropriate expansion parameter for CLF, and fitting the theory at low shear rates to the full theoretical treatment of this problem in the linear regime by Likhtman and McLeish (2002). We obtain

$$\beta_{\mathrm{rcr}}(Z,c_\nu) = [1+0.46\log_{10}(c_\nu)]\left(2.13-\frac{8.91}{\sqrt{Z}}+\frac{12.29}{Z}\right). \tag{27}$$

The above form has been verified against the linear theory in the ranges $Z = 6$–$40$ and $c_\nu = 0.1$–$1$.

### B. Rouse motion on subtube diameter length scales

To capture the correct chain dynamics for times shorter than $\tau_e$ the motion of the chain on length scales less than the tube diameter must be taken into account. We model this using the dynamics of a free Rouse chain. Since the model is applicable only to deformation rates that are small in comparison with $1/\tau_e$ these motions are always in linear response. From this we evaluate the stress contribution as

$$\boldsymbol{\sigma}_{\text{Rouse}}(t) = \int_{\infty}^{t} G(t-t')[\boldsymbol{\kappa}(t') + \boldsymbol{\kappa}(t')^T]dt'. \tag{28}$$

The contribution to $G(t)$ from these Rouse modes is given by Doi and Edwards (1986)

$$G(t) = \frac{G_e}{Z} \sum_{p=Z}^{N} \exp\left(-\frac{2p^2 t}{\tau_R}\right). \tag{29}$$

Generally, this term adds a background viscosity that has a non-negligible contribution when $t \lesssim \tau_e$ or when the number of entanglements is small.

## V. REAL-SPACE SOLUTION

Collecting together the results from the previous sections we obtain a closed system of equations, which is summarized in Table I. The system includes the effects of CLF, retraction, thermal and convective constraint release, and variable number of entanglements. The equations in Table I can be solved numerically and, in a departure from the method of Milner *et al.* (2001), we compute the solution for $\mathbf{f}(s,s')$ via a finite difference scheme in real space rather than using a Fourier series. The computation time for the real space version is $Z$ times faster than the Fourier approach and the form of $\mathbf{f}^{\text{eq}}$ discussed above is more conveniently expressed in terms of real variables. We also note that the approach of Milner *et al.* (2001), in which $\mathbf{f}^{\text{eq}}$ contains a true delta function and the Fourier series is truncated at the tube diameter length scale, leads to some erroneous results. For example when convection and retraction are considered in isolation the solutions fail to produce some known analytic results. If the chain retracts rapidly enough to remain at its equilibrium length then the retraction rate should be exactly $\boldsymbol{\kappa}$:**S**, where **S** is the average orientation of the tube segments. Under shear, this condition becomes

$$\lambda = \frac{5\dot{\gamma}\sigma_{xy}}{12G_e}, \tag{30}$$

since, for an unstretched chain, $\boldsymbol{\sigma} = 12/5G_e\mathbf{S}$. The Fourier solution of the MML model overpredicts the retraction rate in this regime by approximately a factor of 2. Additionally, under these flow condition and in the absence of constraint release, tube segments should become completely aligned in the flow direction at large strains and thus tangent correlations between all points along the chain should saturate. Hence, the function $f_{xx}(s,s')$ should tend to a fixed value for all $s,'s$ as $t \to \infty$. Again, the MML model does not produce this behavior. This indicates that the retraction term produces some motion that acts perpendicularly to the chain contour and so produces some artificial misalignment of the chain. Both of these artifacts tend to produce steady-state shear predictions that are unrealistically high. The problems are due to the sensitivity of the system to the precise implementation of the truncation of the delta functions used by Milner *et al.* (2001). The real space finite difference method outlined above has the correct behavior in both of the above situations and the convergence of the results indi-

**TABLE I.** Closed system of equation including describing the dynamics of an ensemble of entangled linear polymers including: contour length fluctuations, retraction, constraint release, and variable number of entanglements.

Evolution of tangent correlation function

$$\frac{\partial \mathbf{f}}{\partial t} = \boldsymbol{\kappa}\cdot\mathbf{f}+\mathbf{f}\cdot\boldsymbol{\kappa}^{T} \qquad \text{(convention)}$$

$$+\frac{1}{3\pi^2\tau_e}\frac{a}{\sqrt{\mathrm{Tr}\,\mathbf{f}(s_{\min},s_{\min})}}\left(\frac{\partial}{\partial s}+\frac{\partial}{\partial s'}\right)\left(\frac{aD_{\mathrm{CLF}}(s,s')}{\sqrt{\mathrm{Tr}\,\mathbf{f}(s_{\min},s_{\min})}}\left(\frac{\partial}{\partial s}+\frac{\partial}{\partial s'}\right)\mathbf{f}\right) \qquad \text{(reptation + CLF)}$$

$$+\frac{3\nu a}{2}\left[\frac{\partial}{\partial s}\left(\frac{a}{\sqrt{\mathrm{Tr}\,\mathbf{f}(s,s)}}\frac{\partial}{\partial s}(\mathbf{f}-\mathbf{f}^{\mathrm{eq}})\right)+\frac{\partial}{\partial s'}\left(\frac{a}{\sqrt{\mathrm{Tr}\,\mathbf{f}(s',s')}}\frac{\partial}{\partial s'}(\mathbf{f}-\mathbf{f}^{\mathrm{eq}})\right)\right] \qquad \text{(CR)}$$

$$+\frac{\mathcal{R}_s}{2\pi^2\tau_e}\left[\frac{\partial}{\partial s}\left(\mathbf{f}\frac{\partial}{\partial s}\ln[\mathrm{Tr}\,\mathbf{f}(s,s)]\right)+\frac{\partial}{\partial s'}\left(\mathbf{f}\frac{\partial}{\partial s'}\ln[\mathrm{Tr}\,\mathbf{f}(s',s')]\right)\right]. \qquad \text{(retraction)}$$

Equilibrium configuration

$$\mathbf{f}^{\mathrm{eq}}(s,s') = \begin{cases} \frac{1}{3}\mathbf{I} & \text{for } |s-s'| < 1/2 \\ 0 & \text{otherwise} \end{cases}$$

Degree of entanglement

$$Z^*(t) = \frac{1}{a}\int_0^Z \sqrt{\mathrm{Tr}\,\mathbf{f}(s,s)}\,ds$$

CLF diffusion

$$D_{\mathrm{CLF}}(s,s') = \begin{cases} \frac{\alpha_d^2}{s_{\min}^2} & s_{\min} < \alpha_d\sqrt{Z} \\ 1/Z & \text{otherwise} \end{cases}$$

$s_{\min}$ and $\alpha_d$

$$s_{\min} = \mathrm{Min}(s,s',Z-s,Z-s')$$
$$\alpha_d = 1.15$$

$\beta_{\mathrm{rcr}}(Z,c_\nu)$

$$\beta_{\mathrm{rcr}} = (1+0.46\log_{10}(c_\nu))\left(2.13-\frac{8.91}{\sqrt{Z}}+\frac{12.29}{Z}\right)$$

Constraint release rate

$$\nu = c_\nu\left(\lambda+\frac{1}{3\beta_{\mathrm{rcr}}(Z,c_\nu)Z^*(t)Z^2\tau_e}\right)$$

Retraction rate

$$\lambda = -\frac{\mathcal{R}_s}{2aZ^*(t)\pi^2\tau_e}\int_0^Z \frac{1}{\sqrt{\mathrm{Tr}\,\mathbf{f}(s,s)}}\frac{\partial}{\partial s}\left\{\mathrm{Tr}\,\mathbf{f}(s,s')\frac{\partial}{\partial s}\ln[\mathrm{Tr}\,\mathbf{f}(s,s)]\right\}\Big|_{s'=s} ds$$

Stress

$$\boldsymbol{\sigma} = \frac{12G_e}{5Z}\int_0^Z \mathbf{f}(s,s)\,ds+\frac{G_e}{Z}\int_{-\infty}^{t}\sum_{p=Z}^{N}\exp\left(-\frac{2p^2(t-t')}{Z^2\tau_e}\right)[\boldsymbol{\kappa}(t')+\boldsymbol{\kappa}(t')^{\mathrm{T}}]dt'$$

cates their independence from the length-scale truncation of this method of solution. Details of the finite difference scheme are given in Appendix C.

We note that many rheologists are interested only in rheological predictions. For this reason we have developed a single mode equation for the stress tensor based in this model. Details of this work can be found in Likhtman and Graham (2003).

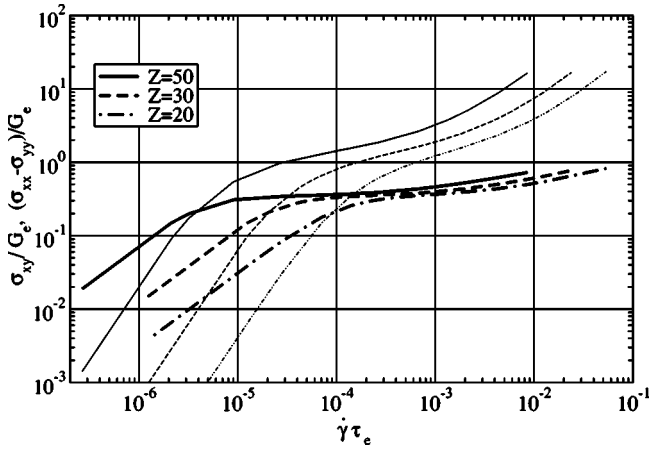


**FIG. 5.** Theory predictions of steady state shear stress (broad lines) and first normal stress difference (thin lines) as a function of shear rate ($c_\nu = 0.1$, $\mathcal{R}_s = 1$).

## VI. RESULTS

The equations in Table I comprise a closed system to determine $\mathbf{f}(s,s')$, which can be solved numerically. From the chain configuration the stress can be obtained via Eq. (4) and with an additional contribution from the unentangled Rouse modes of the chain [Eq. (28)]. A time step of $\sim 0.8\tau_e(Z/N)^2$ was found to give convergent results to within an error of 1% for the parameter ranges we investigated. As discussed above, the results are also independent of the number of points, $N$, for large $N$. All presented results are from converged calculations.

### A. Steady state in shear

Figure 5 shows the steady-state shear stress predictions against shear rate, normalized by $\tau_e$, for a range of values of $Z$. If the curves are plotted with the shear rates expressed in terms of $\dot{\gamma}\tau_R$, where the Rouse time is given by Eq. (13), then the results superimpose at high rates ($\dot{\gamma}\tau_d \gg 1$) where CCR and retraction are the dominant relaxation mechanisms. This holds until $\dot{\gamma}\tau_e \gtrsim 1$, where at these very high rates the assumption that the chains are at equilibrium on length scales less than the tube diameter begins to break down. Note the absence of a shear stress maximum even for a large number of entanglements. The results show a plateau region for shear rates for which $1/\tau_d \ll \dot{\gamma} \ll 1/\tau_R$, where CCR is the dominant relaxation mechanism and the model solutions are self similar. For a comparison with experimental steady-state shear stress data see Fig. 13(a).

### B. Transient startup of simple shear

Figure 6 shows the transient theory predictions from startup of simple shear for a range of shear rates. The transient predictions display a variety of important features. For $\dot{\gamma}\tau_d < 1$ the shear stress is in linear response and normal stress $\sim \dot{\gamma}^2$, neither have overshoots. For $\dot{\gamma}\tau_d \sim 1$ the shear stress has a weak overshoot, while the normal stress remains monotonic. At shear rates around the inverse Rouse time both stresses show overshoots and both the strain at peak stress and the overshoot size increase with shear rate. These features are indicative of chain stretch. At very high rates the stresses exhibit small undershoots before attaining steady state. Similar undershoots have been reported

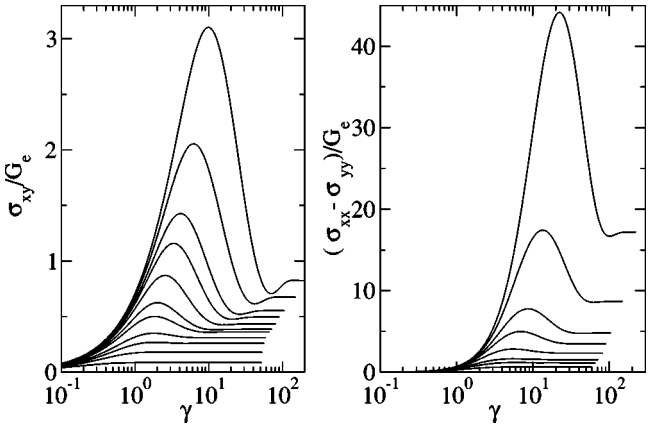


**FIG. 6.** Transient predictions for shear stress and normal stress against strain, $\gamma$, for startup of simple shear. Model parameters: $Z = 20$, $c_\nu = 0.1$, $\mathcal{R}_s = 1$ with shear rates from $\dot{\gamma}\tau_R = 21$ to linear response.

in experimental studies [Osaki *et al.* (2000)]. The transient curves converge rapidly with increasing $N$, with the steady-state value having the slowest convergence.

The assumption of constant tube diameter and persistence length has an interesting effect on the size of the overshoot in the shear stress. Constraint release hastens stretch relaxation and so tends to lower the peak stretch value. It also raises the steady state value through its influence on orientation. The net effect is to reduce the size of the stress overshoot, measured by the ratio of the maximum shear stress to the steady state value. However, the renormalisation of the influence of CCR, resulting from the assumption of a constant tube persistence length, acts to weaken the action of CCR on an extended chain. Thus, for the calculations in Fig. 6 the overshoot size grows with increasing shear rate in agreement with trends seen experimentally. Alternatively, if the assumption that the number of entanglement segments remains fixed even in a stretched chain is made, the modification of Eq. (8) must be omitted. In this case, the theory predicts that the overshoot size remains relatively modest, even at very high shear rates, resulting in predicted overshoots that are too weak to explain the widely observed experimental values. A similar difficulty was reported for the model of Mead *et al.* (1998) by Pattamaprom and Larson (2001) and this may be attributed to the lack of CCR-stretch renormalization in their model.

Due to the decoupling approximation in Eq. (16) our model predicts a zero value for the second normal stress difference. This is a clear disadvantage when compared to the Doi–Edwards model. However, the experimental values of the second normal stress difference are, typically, very small relative to other components of the stress tensor and are exceptionally difficult to measure. We believe that in order to make reliable predictions of the second normal stress difference, one needs to solve Eq. (12) without any decoupling approximations.

### C. Damping function

The model's predictions of the relaxation function after a large step strain, $G(t,\gamma) = \sigma_{xy}/\gamma$, are time-strain separable in the following way

$$G(t,\gamma) = h(\gamma)G(t), \tag{31}$$

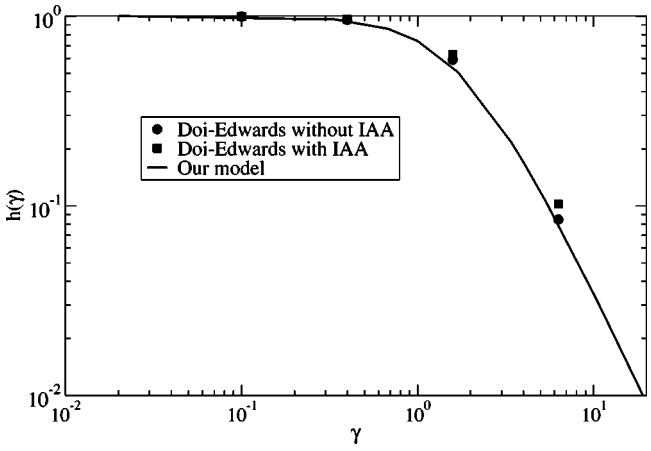


**FIG. 7.** Comparison of our model predictions for the damping function with those of the Doi–Edwards model with and without the independent alignment approximation (IAA).

at long times. Consequently, a comparison with the predictions of Doi–Edwards model for the damping function, $h(\gamma)$, can be made. Figure 7 shows that the predictions of the two models are very close and, since the Doi–Edwards model is known to be in good agreement with experimental data for this measurement, we conclude that the our model will also successfully capture such data.

### D. Single chain structure factor

The single chain structure factor, $S(\mathbf{q})$, for an entangled liquid under strong flow can be obtained from the chain configuration through Eq. (5). Figure 8 shows contour plots of a melt under steady shear for a range of shear rates The plots are for a moderately nonlinear flow rate, a rate on the plateau, and a stretching flow both with and without contour length fluctuations. The angle made by the major axis of each elliptical contour gives an indication of the degree of chain alignment. For the slowest flow $S(\mathbf{q})$ is only weakly perturbed from an isotropic distribution. The plots corresponding to $\dot{\gamma}\tau_d = 25$ show most clearly the variation in degree of chain alignment with length scale. Contour length fluctuations reduce the degree of alignment in each case and distorts the isointensity curves away from an elliptic shape. These plots indicate the usefulness of resolving the chain contour down to the length scale of the tube diameter and the additional information that is provided by this approach. Future small angle neutron scattering (SANS) data on sheared, well-entangled polymer melts will constrain theory is ways that measurements of stress alone are unable to do.

## VII. COMPARISON WITH EXPERIMENTAL DATA

In this section we compare our theoretical predictions with a range of experimental data sets for entangled solutions of nearly monodisperse linear polymers from the literature [Menezes and Graessley (1982); Menezes (1980); Kahvand (1995); Hua *et al.* (1999); Osaki *et al.* (2000); Pattamaprom and Larson (2001); Ye *et al.* (2003)]. For each set both linear oscillatory shear and nonlinear shear measurements, including viscosity and first normal stress difference, both to steady state, are available. In some cases measurements were made for a range of molecular weights at fixed monomer concentration. This enables a direct test of the hypothesis that the model parameters should be independent of molecular weight. In all cases the polymer concentration was carefully

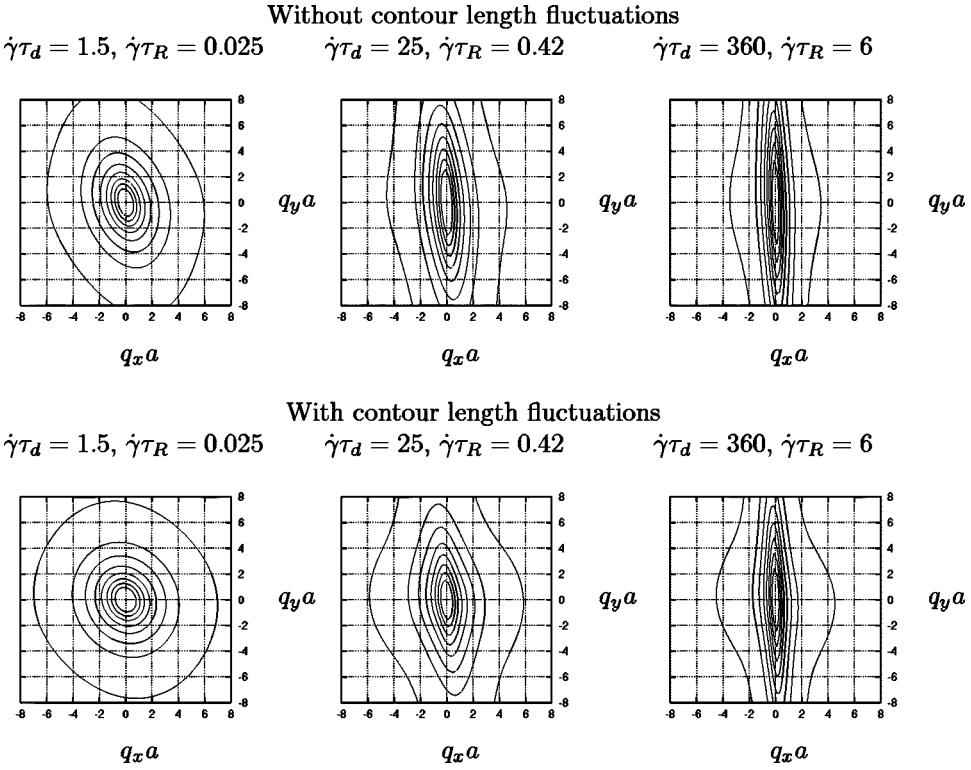


**FIG. 8.** $S(\mathbf{q})$ in steady shear for a range of shear rates. Model parameters: $Z = 20$, $c_\nu = 0.1$, and $\mathcal{R}_s = 1$. Contours lines map the same value on each plot.

chosen to minimize elastic instabilities while maximising the degree of entanglement. The material details are summarized in Tables II and III.

## A. Determination of model parameters

The model requires five parameters $G_e$, $\tau_e$, $M_e$, $c_\nu$, and $\mathcal{R}_s$. The first three of these are specified by the linear rheology of the material and each is expected to vary with chemistry and monomer concentration but not with molecular weight. The remaining two parameters, $\mathcal{R}_S$ and $c_\nu$, are dimensionless prefactors for the retraction and constraint release terms, respectively. We set these parameters to universal values since entangled

**TABLE II.** Parameters for two polybutadiene solutions used by Menezes and Graessley (1982) at fixed monomer concentration. Material parameters are as quoted in the original papers, linear parameters are obtained from linear oscillatory shear and calculated parameters are computed from the other parameters.

| Material values | | | | Linear parameters | | | | Calculated params. | |
|---|---|---|---|---|---|---|---|---|---|
| Material | $M_w$ kg mol$^{-1}$ | Conc. | $M_w/M_n$ | $G_e$ Pa | $\tau_e$ $\times 10^{-3}$ s | $M_e$ kg mol$^{-1}$ | $c_\nu$ | $Z$ | $\tau_R$ s |
| PBB | 350 | 7% | $< 1.05$ | 51779 | 4.156 | 42.7 | 0.1 | 8 | 0.266 |
| PBD | 813 | 7% | $< 1.05$ | 51779 | 4.156 | 42.7 | 0.1 | 19 | 1.50 |

**TABLE III.** Material parameters for a range of polystyrene solutions: PS/TCP [Kahvand (1995)], f128-10 [Osaki *et al.* (2000)], 2.89 and 8.42 M [Pattamaprom and Larson (2001)]. Parameters are obtained by the algorithm described in the text.

| Material values | | | | Linear parameters | | | | Calculated params. | |
|---|---|---|---|---|---|---|---|---|---|
| Material | $M_w$ kg mol$^{-1}$ | Conc. | $M_w/M_n$ | $G_e$ Pa | $\tau_e$ $\times 10^{-3}$ s | $M_e$ kg mol$^{-1}$ | $c_\nu$ | $Z$ | $\tau_R$ s |
| PS/TCP | 1900 | 13% | 1.2 | 23711 | 7.755 | 158 | 0.1 | 12 | 1.117 |
| f128-10 | 1090 | 10% | sharp | 1302 | 51.42 | 136 | 0.1 | 8 | 3.29 |
| 2.89 M | 2890 | 7% | 1.09 | 8075 | 1.911 | 270 | 0.1 | 11 | 0.23 |
| 8.42 M | 8420 | 7% | 1.14 | 8075 | 1.911 | 270 | 0.1 | 31 | 1.836 |

polymers are believed to be governed by universal underlying dynamics. Thus, these two parameters cannot be tuned to individual data sets. Arguments leading to numerical values for these two dimensionless parameters are presented below.

The three linear parameters: $G_e$, $\tau_e$ and $M_e$, are found by fitting the linear theory of Likhtman and McLeish (2002) to linear oscillatory shear measurements. We suggest that simultaneously fitting several molecular weights leads to more accurate values. The parameters obtained for two polybutadiene solutions, PBB and PBD, are shown in Table II. In principle, it is possible to compute the value of $M_e$ for a solution from its melt value using a relationship for the scaling with concentration, $c$,

$$M_e(c) = M_e^{\text{melt}} c^{\alpha}. \tag{32}$$

However, the scaling exponent, $\alpha$, has yet to be decisively determined. The two most commonly used values for this exponent are 1 and 4/3. We verified that each of our diluted values of $M_e$, throughout this paper, are consistent with $1 < \alpha < 4/3$ by using the melt values of $M_e$ for polybutadiene and polystyrene from Likhtman and McLeish (2002).

We continue with arguments leading to universal values for the parameters $c_\nu$ and $\mathcal{R}_s$. The value of $c_\nu$ determines the number of retraction events necessary to produce one tube hop of length $a$. The quality of agreement with the linear data is not strongly dependent on $c_\nu$ and provided it is in the range 0.1–1 good agreement with the complex modulus data is found (see Fig. 9). Thus, $c_\nu$ cannot be cleanly specified by linear rheology and so

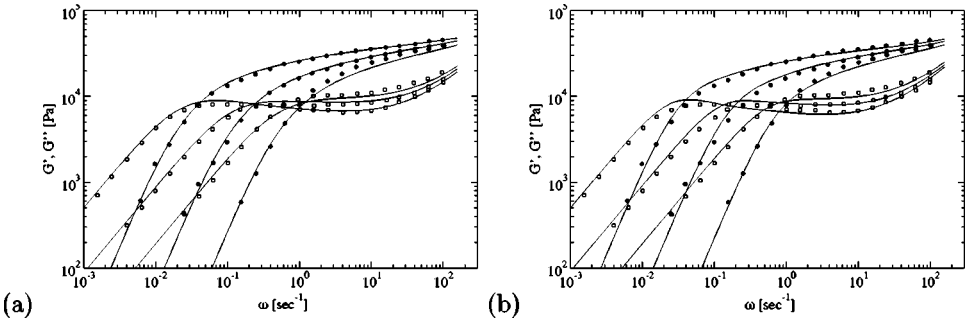


**FIG. 9.** Comparison with the Menezes and Graessley (1982) linear oscillatory shear data for three polybutadiene solutions: PBB, PBC ($M_w = 517$ k) and PBD, with $c_\nu = 1.0$ (a) and $c_\nu = 0.1$ (b). Model parameters, listed in Table II, are the same for each molecular weight.

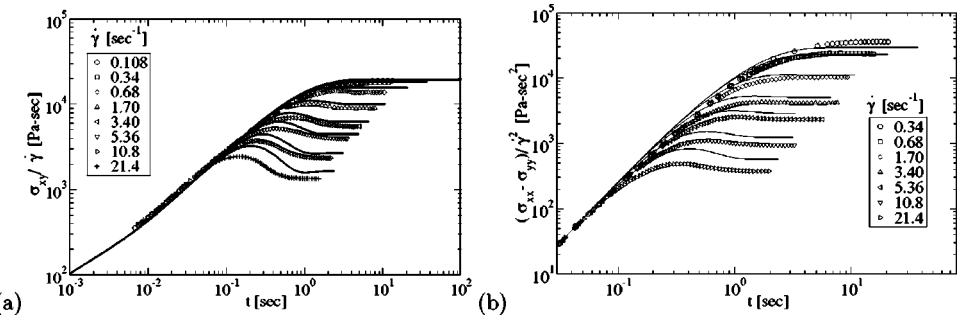


**FIG. 10.** Comparison with Menezes and Graessley (1982) PBB shear viscosity (a) and first normal stress difference (b) data using parameters obtained only from linear rheology and $\mathcal{R}_s = 1$.

we fix its value by the following argument. Milner *et al.* (2001) indicated that $c_\nu \lesssim 1$ and they demonstrated that a value greater than 0.06 was sufficient to remove the shear stress maximum. Thus, to choose from inside this range, we set $c_\nu = 0.1$ since values closer to order 1 produce smaller shear stress overshoots than are seen experimentally. The final parameter, $\mathcal{R}_s$, accounts for the decoupling approximation in the retraction term. To proceed we initially set this value to unity.

In table II the calculated parameters are not free. The value of $M_e$ fixes the number of entanglements, $Z$, for a particular molecular weight via $Z = M_w/M_e$ and the Rouse time is given by $\tau_R = Z^2\tau_e$. The Rouse time in not directly inserted into the model and is shown merely to allow a convenient calculation of the stretching Weissenberg number, $\dot{\gamma}\tau_R$.

### B. Parameter free comparison with nonlinear data

In the algorithm described above all model parameters are either set to universal values or are obtained from linear oscillatory shear measurements. Thus, a parameter free comparison with the nonlinear data can be made. The results for transient shear and normal stresses of PBB are shown in Fig. 10. The agreement with the moderately nonlinear rates ($\dot{\gamma} = 0.34$–$3.40\ \mathrm{s}^{-1}$) is good. However, the model overpredicts the peak stress value at the higher shear rates. Similar results are obtained for both transient viscosity and first normal stress difference for PBD. In both cases the agreement is good for the nonlinear rates $1/\tau_d \lesssim \dot{\gamma} < 1/\tau_R$ but the predicted peak stress value is too large for shear rates in excess of the inverse Rouse time.

In Fig. 10 the early time predictions ($t < \tau_e$) have a slope that is less than one. This is a direct manifestation of the entangled Rouse modes which are described in Sec. IV B. These modes are more prominent for the PBB predictions than the other materials since the number of entanglements is relatively low.

### C. Improvement of high rate predictions

The results of the previous section suggest that the model is effective for nonlinear flows that do not stretch the chain. However, the overprediction of the peak stress value indicates that, with $\mathcal{R}_s = 1$, the model accumulates too much chain stretch at the highest shear rates. To remedy this discrepancy we revise the value of the order one prefactor, $\mathcal{R}_s$. This parameter accounts for the decoupled retraction term in Eq. (18) and increasing its value enhances the retraction rate. $\mathcal{R}_s$ is chosen by fitting the highest experimental rate of the PBB shear viscosity data. A value of $\mathcal{R}_s = 2.0$ gives best fit to the $\dot{\gamma} = 21.4$

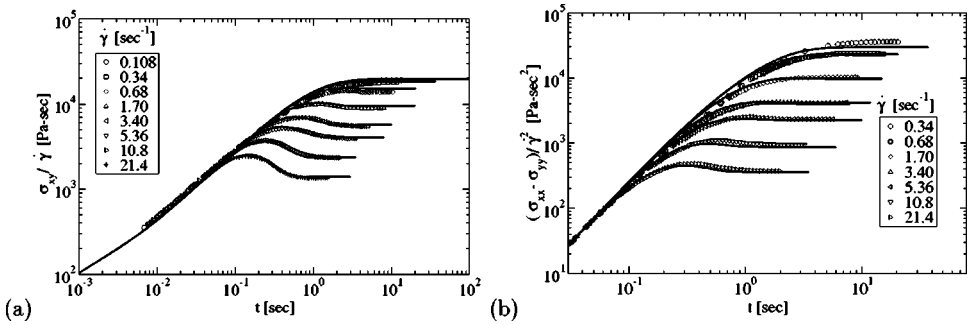


**FIG. 11.** Comparison with Menezes and Graessley (1982) PBB shear viscosity (a) and first normal stress difference (b) data using parameters obtained from linear rheology and $\mathcal{R}_S = 2.0$.

transient curve. The results for all rates are shown in Fig. 11 along with the normal stress comparison. Adjusting this single universal parameter produces good agreement across all of the measured rates for both shear and normal stresses. We use $\mathcal{R}_S = 2.0$ for *all* subsequent calculations in this paper.

The generality of this universal value of $\mathcal{R}_S$ is demonstrated by Fig. 12, in which data and theory for PBD are compared. The universal values are now fixed and the molecular weight independent parameters from Table II are used. Even though the algorithm allows no variation of the model parameters the agreement between data and theory is good. Below we will discuss the areas of slight disagreement in the context of a wider data comparison.

### D. Further entangled solutions

At this point our algorithm for parameter determination is fixed. We always set $c_\nu = 0.1$ and $\mathcal{R}_S = 2.0$ and the remaining three linear parameters are obtained by fitting to linear oscillatory shear measurements, subject the constraint that they should be independent of molecular weight. There is no freedom to vary the approach for each data set. We are now in a position to test the robustness of this method by comparing with a broad range of literature data. We compare with non-linear shear data from a further three publications: Kahvand (1995); Osaki *et al.* (2000); Pattamaprom and Larson (2001). The linear parameters for these materials are contained in Table III; as before these parameters were obtained by fitting the linear theory of Likhtman and McLeish (2002) to linear oscillatory shear data. The resulting nonlinear data comparisons are shown in Figs. 13–15.

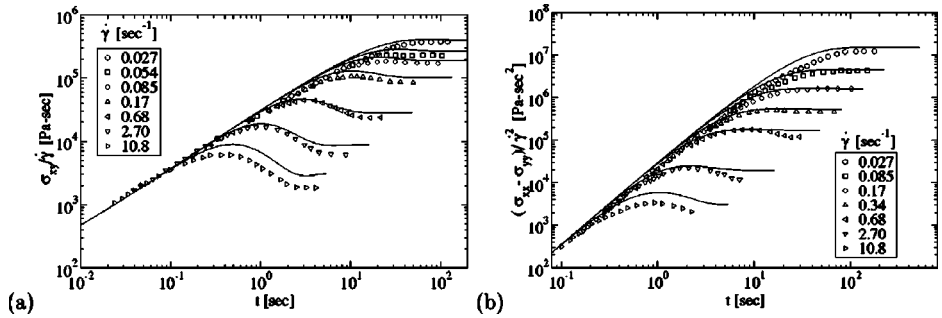


**FIG. 12.** Comparison with Menezes and Graessley (1982) PBD shear viscosity (a) and first normal stress difference (b) data using parameters obtained from linear rheology and $\mathcal{R}_S = 2.0$.

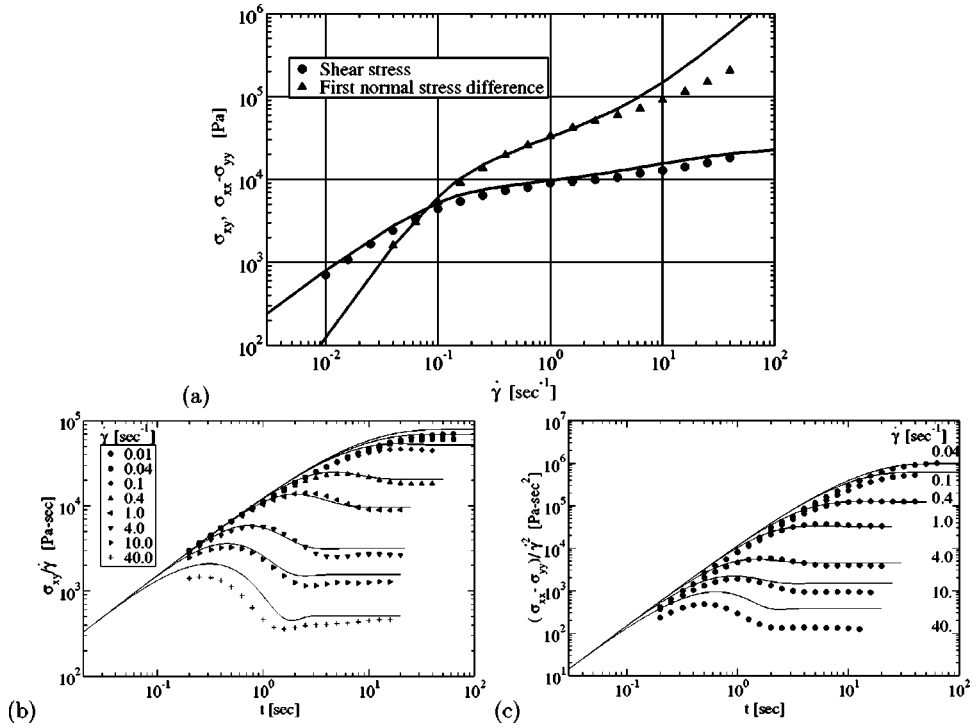


**FIG. 13.** Comparison with Kahvand (1995) PS/TCP shear viscosity and first normal stress difference in steady state (a) and transient plots (b), and (c).

All plots show good agreement between theory and experiment over a wide range of shear rates, particularly considering the complete absence of non-linear parameter fitting for these plots. For most rates the peak stress value, the time of peak stress and the steady-state value are successfully predicted for both shear stress and first normal stress difference. Especially encouraging is that the model appears to capture the rheological behavior of a wide range of polymer fluids through an underlying theory for universal nonlinear dynamics of these entangled polymers. If the linear rheology of a material is known the model is able to make quantitative predictions for nonlinear flow. Furthermore, since the linear parameters are molecular weight independent, the model can ac-

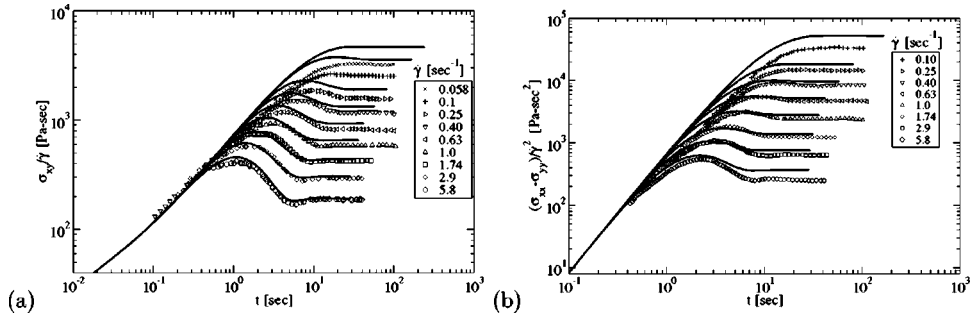


**FIG. 14.** Comparison with Osaki *et al.* (2000) f128-10 shear viscosity (a) and first normal stress difference (b) data.

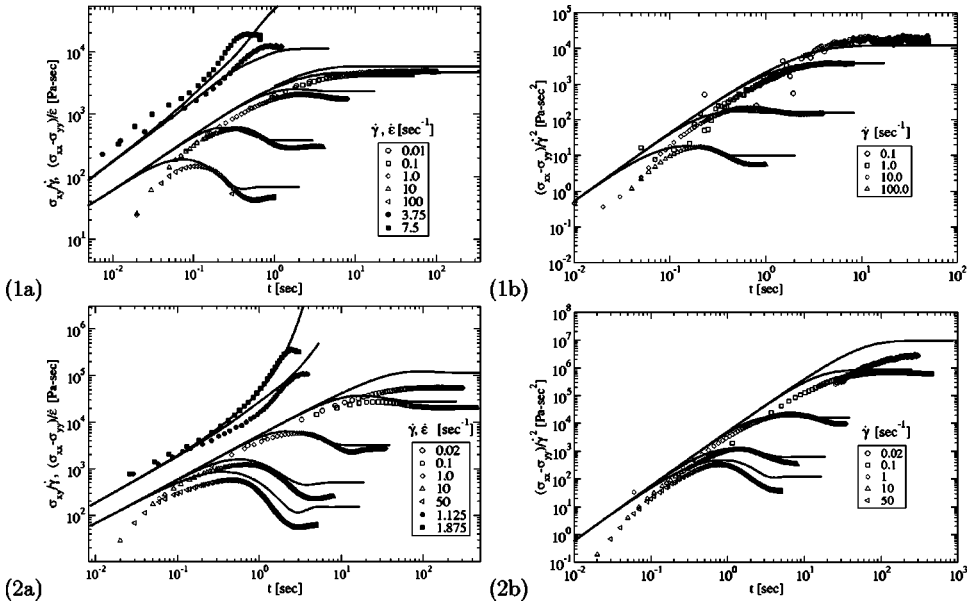


**FIG. 15.** Comparison with shear rheology data by Pattamaprom and Larson (2001) and uniaxial extension data by Ye *et al.* (2003) for 2.89 M (1) and 8.42 M (2) both with shear and extension viscosity (a) and first normal stress difference under shear (b). The extensional data have been shifted to the same temperature as the shear data.



curately predict variations due to molecular weight. The algorithm is successful despite variations in the degree of entanglement, monomer concentration, and chemical composition in the experimental data.

There are, however, some areas of systematic disagreement. At the highest available deformation rates there is an overprediction of the steady state stress and, to a lesser extent, the peak stress values. This is particularly true of the normal stress at these very large rates. This effect occurs at deformation rates of $\dot{\gamma}\tau_R \gtrsim 15 \sim 20$ for all sets that achieve these high Weissenberg numbers. The steady-state normal stress comparison in Fig. 13(a) demonstrates this onset most clearly and indicates that the model predicts too much stretching in this regime. However for $\dot{\gamma}\tau_R \lesssim 15$ the universality of our choice for $\mathcal{R}_s$ is clearly evident. The disagreement for times $< 0.1$ s with the data of Pattamaprom and Larson (2001) is due to a communication delay between the motor and transducer as acknowledged in the original paper.

We have already advanced one explanation for the need for the parameter $\mathcal{R}_s$: that it results from the closure approximation used in the retraction term. It is known that this type of closure can lead to errors of order one, which would account for the necessary prefactor. This could be resolved by comparing the solutions of the closed equations with stochastic simulations of Eq. (12). An alternative explanation is that the method of determination of the Rouse time from the linear rheology is relatively indirect. This time scale dominates the nonlinear regime, yet it must be inferred from a knowledge of the terminal behavior of the material in linear shear. This region of the complex modulus is controlled by a combination of CLF, reptation and constraint release, and the reliability of this method for obtaining the Rouse time depends on the implementation of these processes in the relevant linear theory. Finally, it is possible that the model omits a physical process that acts to accelerate chain retraction inside a tube. One possibility would be to

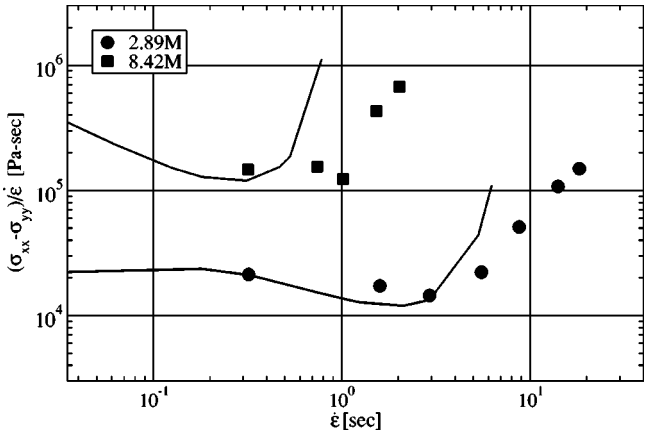


**FIG. 16.** Comparison with Ye *et al.* (2003) steady state uniaxial extension data for 2.89 and 8.42 M. The model has no steady state value for $\dot{\epsilon}\tau_R \gtrsim 1$ since it omits chain finite extensibility effects. Experimental data are shifted to 40 °C.

change our assumptions about deformation of the tube under flow, as discussed in Sec. III B. However, it is not obvious how this would lead to faster chain retraction. This issue may also explain the overprediction of the peak stress values at very large shear rates as seen in the data comparison.

### E. Extensional flow

The two solutions used by Pattamaprom and Larson (2001) have also been recently characterized in nonlinear uniaxial extension by Ye *et al.* (2003). We used the time–temperature superposition shift factors from linear rheology to reduce the extensional data to the same temperature as the shear rheology and a comparison with the transient data is shown in Fig. 15. For these calculations the model parameters are identical to those used for the shear calculations; only the deformation tensor has been changed. Significantly, the model also shows reasonable agreement with the transient extension curves. It certainly does not systematically under or overpredict of the degree of chain stretching and the agreement between the 8.42 M data and theory for the $\dot{\epsilon} = 1.875\ \mathrm{s}^{-1}$ transient is particularly close. This suggests that our chosen value of $\mathcal{R}_s = 2.0$ is also applicable to extensional flows. A comparison with the steady-state data is shown in Fig. 16 and the model is in reasonable agreement at rates for which $\dot{\epsilon}\tau_R \lesssim 1$. In particular, the model correctly predicts the degree of strain softening at weakly non-linear rates. The model fails in steady state at high extension rates since our assumption that the chain spring constant is linear in invalid in this region. At large strains in rapid extension deformations finite extensibility of the chain contour becomes significant and this effect controls the experimental steady state value.

## VIII. CONCLUSIONS

The model presented in this paper contains a series of refinements to the Doi–Edwards model of reptation in entangled linear polymers that extend it into the strongly nonlinear regime of chain stretch. In addition to reptation, the effects of finite rate retraction and convective constraint release are included. All of these processes are accounted for in a microscopic stochastic partial differential equation for the motion of the chain contour

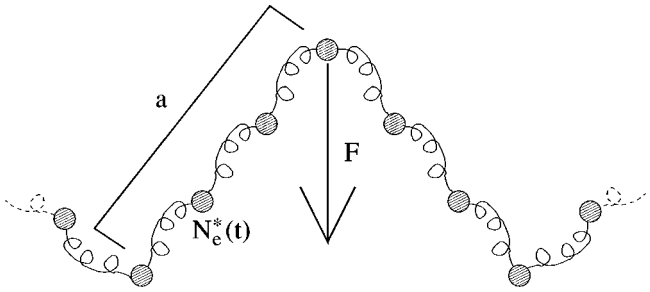


**FIG. 17.** Derivation of CCR term for a stretched chain.

from which the model is derived. In particular, CCR is treated as a *local* relaxation and excitation of the tube. Real-space solutions of the model in strong shear indicate the absence of a steady-state maximum in the shear stress. Through this detailed local treatment of relaxation it is possible to predict not only mechanical stresses but also single chain structure factor under flow. Also, included is chain stretch which considerably improves the transient predictions for rapid deformations. In addition, we have considered the tube diameter to be fixed even under strong flow as opposed to an assumption of a constant number of entanglements per chain. Our assumption leads to a weakening of the influence of CCR when the chain is stretched, improving the size of the predicted stress overshoot in shear compared to the model of Mead *et al.* (1998), which omits this mechanism. The experimental observation of large overshoots supports the assumption that the tube diameter is not strongly perturbed from its equilibrium value by deformation rates up to several times the inverse Rouse time of the chain.

An accurate comparison with a broad range of experimental data in nonlinear shear, encompassing many different entangled solutions, was made. All model parameters were either fixed by linear oscillatory shear measurements or were set to universal values with no non-linear fitting to individual data sets. With no parameter adjustment the model was shown to be in reasonable agreement with extensional measurements made on one of the investigated materials.

The physical origin of all the model parameters is clear except for the prefactor to the retraction term, $\mathcal{R}_s$, which is shown to optimize predictions uniformly across all available data sets with a value of 2.0. The value of this universal number may attributed to either the decoupling approximations used to produce a closed equation or missing physics from the model derivation. Further work and a complimentary investigation of the decoupling approximations will be necessary to resolve this issue.

## APPENDIX A: DERIVATION OF STRETCH-CCR RENORMALIZATION TERM

In this appendix we derive the modification of the constraint release term in the MML model to include the effect of chain stretch. In the MML model the Rouse-like CCR term was derived by considering the motion of a Brownian particle moving between a series of obstacles which disappear and reappear with frequency $\nu$ and subject to an effective potential which depends on the chain spring constant [see Graham (2002) for details of this derivation]. We assume that the tube diameter is fixed under deformation and recompute the effective potential for a stretched chain to obtain a generalized CCR term (Fig. 17). In equilibrium there are $N_e$ monomers per tube segment and as the chain stretches this number reduces in proportion with the local stretch. Thus, at any instant in time the tube segment at position $s$ will contain

$$N_e^*(s,t) = \frac{a}{|\mathbf{R}'(s)|} N_e$$

monomers. Treating the tube segment as a Gaussian chain of $N_e^*$ monomers, gives the spring force acting on that tube segment as

$$\boldsymbol{\mathcal{F}} = -\frac{3k_BT}{N_e^*(t)b^2}(\mathbf{R}_n - \mathbf{R}_{n+N_e^*(t)} + \mathbf{R}_n - \mathbf{R}_{n-N_e^*(t)}), \tag{33}$$

which, in the continuous limit, becomes

$$\boldsymbol{\mathcal{F}} = \frac{3k_BT}{N_e^*(t)b^2} N_e^*(t)^2 \frac{\partial^2 \mathbf{R}}{\partial n^2}, \tag{34}$$

rescaling in terms of the tube variable, $s$ gives

$$\boldsymbol{\mathcal{F}} = \frac{3k_BT}{a^2} \frac{a}{|\mathbf{R}'(s)|} \frac{\partial^2 \mathbf{R}}{\partial s^2}. \tag{35}$$

In the derivation of Milner *et al.* (2001) the term corresponding to Rouse-like tube motion is $(\nu a^2/2k_BT)\boldsymbol{\mathcal{F}}$ which leads to the required result.

$$\frac{\partial \mathbf{R}}{\partial t} = \cdots + \frac{3\nu}{2} \frac{a}{|\mathbf{R}'(s)|} \mathbf{R}''(s). \tag{36}$$

## APPENDIX B: MODIFIED CLF TERM FOR A STRETCHED CHAIN

In one dimension the contour variable diffusion equation is

$$\frac{\partial \mathbf{f}}{\partial t} = \frac{\partial}{\partial s}\left( D(s) \frac{\partial}{\partial s} \mathbf{f}(s) \right). \tag{37}$$

However, when the chain is stretched this form artificially accelerates the relaxation. The diffusion should occur a fixed rate in real space, $x$, not monomer space. Thus a more general form is

$$\frac{\partial \mathbf{f}}{\partial t} = \frac{\partial}{\partial x}\left( D(s) \frac{\partial}{\partial x} \mathbf{f}(s) \right) = \frac{ds}{dx} \frac{\partial}{\partial s}\left( D(s) \frac{ds}{dx} \frac{\partial}{\partial s} \mathbf{f}(s) \right). \tag{38}$$

Using $ds/dx = a/|\mathbf{R}'(s)|$, we obtain

$$\frac{\partial \mathbf{f}}{\partial t} = \frac{a}{|\mathbf{R}'(s)|} \frac{\partial}{\partial s}\left( D(s) \frac{a}{|\mathbf{R}'(s)|} \frac{\partial}{\partial s} \mathbf{f}(s) \right), \tag{39}$$

which we generalize into two dimensions:

$$\frac{\partial \mathbf{f}}{\partial t} = +\frac{1}{3\pi^2 \tau_e} \frac{a}{\sqrt{\mathrm{Tr}\,\mathbf{f}(s_{\min}, s_{\min})}} \left( \frac{\partial}{\partial s} + \frac{\partial}{\partial s'} \right) \frac{aD_{\mathrm{CLF}}(s,s')}{\sqrt{\mathrm{Tr}\,\mathbf{f}(s_{\min}, s_{\min})}} \left( \frac{\partial}{\partial s} + \frac{\partial}{\partial s'} \right) \mathbf{f}. \tag{40}$$

The influence of this renormalization of the CLF term with stretch is generally minimal since the chain stretch is small near the chain ends where the fluctuations are most significant.

## APPENDIX C: FINITE DIFFERENCE SOLUTION OF THE MODEL

To obtain a real space solution we subdivide the chain into $N+1$ points and define the function

$$\mathbf{f}_{[p,q]} = \frac{1}{a^2}\mathbf{f}\left(\frac{pZ}{N}, \frac{qZ}{N}\right), \tag{41}$$

for $p,q = 0–N$. The boundary conditions are $\mathbf{f}_{[p,q]} = \mathbf{f}^{\mathrm{eq}}_{[p,q]}$, on the the perimeter of the area given by $p,q = 0–N$, at all times. A coupled system of $(N-1)^2$ ordinary differential equations for the remaining $\mathbf{f}_{[p,q]}$ is obtained from Eq. (18) using following finite difference scheme for all derivatives with respect to $s$ and $s'$. First and second order derivatives are defined as follows:

$$\begin{aligned}\frac{\partial}{\partial s}(\mathbf{f}_{[p,q]}) &= \frac{N}{2Z}(\mathbf{f}_{[p+1,q]} - \mathbf{f}_{[p-1,q]}),\\ \frac{\partial^2}{\partial s^2}(\mathbf{f}_{[p,q]}) &= \left(\frac{N}{Z}\right)^2 (\mathbf{f}_{[p+1,q]} + \mathbf{f}_{[p-1,q]} - 2\mathbf{f}_{[p,q]}),\end{aligned} \tag{42}$$

and the following derivatives are needed for the CLF term:

$$\begin{aligned}\left(\frac{\partial}{\partial s} + \frac{\partial}{\partial s'}\right)\mathbf{f}_{[p,q]} &= \frac{N}{2Z}(\mathbf{f}_{[p+1,q+1]} - \mathbf{f}_{[p-1,q-1]}),\\ \left(\frac{\partial}{\partial s} + \frac{\partial}{\partial s'}\right)^2\mathbf{f}_{[p,q]} &= \left(\frac{N}{Z}\right)^2 (\mathbf{f}_{[p+1,q+1]} + \mathbf{f}_{[p-1,q-1]} - 2\mathbf{f}_{[p,q]}).\end{aligned} \tag{43}$$

Equation (18) can be used to describe the time evolution of all internal points ($p,q = 1–N-1$) since all finite difference derivatives can be evaluated for these points. Integrals are evaluated using the trapezium rule. Thus,

$$\int_0^Z \mathcal{F}(s)ds \approx \frac{Z}{2N}\left[\mathcal{F}(0) + \mathcal{F}(Z) + 2\sum_{p=1}^{N-1}\mathcal{F}\left(\frac{pZ}{N}\right)\right]. \tag{44}$$

The function $\mathbf{f}^{\mathrm{eq}}$ is written in terms of the discrete variables according to Eq. (19) and it is important that the following integral conditions for $\mathbf{f}^{\mathrm{eq}}$ hold:

$$\int_0^Z \mathrm{Tr}\,\mathbf{f}^{\mathrm{eq}}(s,s')ds' = 1, \quad \int_0^Z \mathrm{Tr}\,\mathbf{f}^{\mathrm{eq}}(s,s)ds = Z. \tag{45}$$

The exact derivatives of $D_{\mathrm{CLF}}$ can be defined in terms of generalized step functions, however, it is more convenient, in practise, to use a small finite step in $s,s'$, to approximate the derivatives of $D_{\mathrm{CLF}}$. If the step, $\epsilon$, is sufficiently small ( $\sim 10^{-2}$) the results are independent of $\epsilon$ since this definition formally exact in the limit $\epsilon \to 0$.

## ACKNOWLEDGMENTS

The authors thank EPSRC for funding the ''Microscale Polymer Processing'' project, during which this work was carried out. The authors also thank the Kavli Institute for Theoretical Physics in Santa Barbara, where part of this work was performed with partial support from the National Science foundation under Grant No. PHY99-07949. One of the authors (R.S.G.) acknowledges funding from the EPSRC under a CASE award sponsored

by BP Chemicals. The authors thank David Venerus, Professor Osaki, Ron Larson, and Tam Sridhar for kindly making their experimental data available to them. The authors are grateful for very helpful discussions at many points of this work, and insightful comments and suggestions from Daniel Read, Oliver Harlen, and Ron Larson.

## References

Bercea, M., C. Peiti, B. Simionescu, and P. Navard, ''Shear rheology of semidilute poly(methyl methacrylate) solutions,'' Macromolecules **26**, 7095–7096 (1993).

de Gennes, P.-G., ''Reptation of stars,'' J. Phys. (Paris) **36**, 1199–1202 (1975).

Doi, M. and S. F. Edwards, *The Theory of Polymer Dynamics* (Oxford University Press, Oxford, U.K., 1986).

Graham, R. S., Ph.D. thesis, University of Leeds (2002).

Hua, C. C., J. D. Schieber, and D. C. Venerus, ''Segment connectivity, chain-length breathing, segmental stretch, and constraint release in reptation models. III. Shear flows,'' J. Rheol. **43**, 701–717 (1999).

Ianniruberto, G., and G. Marrucci, ''On compatibility of the Cox–Merz rule with the model of Doi and Edwards,'' J. Non-Newtonian Fluid Mech. **65**, 241–246 (1996).

Ianniruberto, G., and G. Marrucci, ''Convective orientational renewal in entangled polymers,'' J. Non-Newtonian Fluid Mech. **95**, 363–374 (2000).

Ianniruberto, G., and G. Marrucci, ''A simple constitutive equation for entangled polymers with chain stretch,'' J. Rheol. **45**, 1305–1318 (2001).

Kahvand, H., Ph.D. thesis, Illinois Institute of Technology (1995).

Likhtman, A. E., and R. S. Graham, ''Simple constitutive equation for linear polymer melts derived from molecular theory: Rolie poly equation,'' J. Non-Newtonian Fluid Mech. (in press).

Likhtman, A. E., and T. C. B. McLeish, ''Quantitative theory for linear dynamics of linear entangled polymers,'' Macromolecules **35**, 6332–6343 (2002).

Likhtman, A. E., S. T. Milner, and T. C. B. McLeish, ''Microscopic theory for the fast flow of polymer melts,'' Phys. Rev. Lett. **85**, 4550–4553 (2000).

Marrucci, G., ''Dynamics of entanglements: A nonlinear model consistent with the Cox–Merz rule,'' J. Non-Newtonian Fluid Mech. **62**, 279–289 (1996).

Marrucci, G., and N. Grizzuti, ''Fast flows of concentrated polymers—predictions of the tube model on chain stretching,'' Gazz. Chim. Ital. **118**, 179–185 (1988).

McLeish, T. C. B., ''Tube theory of entangled polymer dynamics,'' Adv. Phys. **51**, 1379–1527 (2002).

McLeish, T. C. B., J. Allgaier, D. K. Bick, G. Bishko, P. Biswas, R. Blackwell, B. Blottière, N. Clarke, B. Gibbs, D. J. Groves, A. Hakiki, R. K. Heenan, J. M. Johnson, R. Kant, D. J. Read, and R. N. Young, ''Dynamics of entangled H polymers: Theory, rheology, and neutron scattering,'' Macromolecules **32**, 6734–6758 (1999).

Mead, D. W., R. G. Larson, and M. Doi, ''A molecular theory for fast flows of entangled polymers,'' Macromolecules **31**, 7895–7914 (1998).

Mead, D. W., and L. G. Leal, ''The reptation model with segmental stretch basic equations and general properties,'' Rheol. Acta **34**, 339–359 (1995).

Menezes, E. V., Ph.D. thesis, Northwestern University (1980).

Menezes, E. V., and W. W. Graessley, ''Nonlinear rheological behavior of polymer systems for several shear-flow histories,'' J. Polym. Sci., Part B: Polym. Phys. **20**, 1817–1833 (1982).

Milner, S. T., T. C. B. McLeish, and A. E. Likhtman, ''Microscopic theory of convective constraint release,'' J. Rheol. **45**, 539–563 (2001).

Müller, R. C., J. J. Pesce, and C. Picot, ''Chain conformation in sheared polymer melts as revealed by SANS,'' Macromolecules **26**, 4356–4362 (1993).

Osaki, K., T. Inoue, and T. Isomura, ''Stress overshoot of polymer solutions at high rates of shear,'' J. Polym. Sci., Part B: Polym. Phys. **38**, 1917–1925 (2000).

Pattamaprom, C., and R. G. Larson, ''Constraint release effects in monodisperse and bidisperse polystyrenes in fast transient shearing flows,'' Macromolecules **34**, 5229–5237 (2001).

Pattamaprom, C., R. G. Larson, and T. J. Van-Dyke, ''Quantitative predictions of linear properties of entangled polymers,'' Rheol. Acta **39**, 517–531 (2000).

Pearson, D., E. Herbolzheimer, N. Grizzuti, and G. Marrucci, ''Transient behavior of entangled polymers at high shear rates,'' J. Polym. Sci., Part B: Polym. Phys. **29**, 1589–1597 (1991).

Rubinstein, M., and R. H. Colby, ''Self-consistent theory of polydisperse entangled polymers–linear viscoelasticity of binary blends,'' J. Chem. Phys. **89**, 5291–5306 (1988).

Rubinstein, M., and S. Panyukov, ''Nonaffine deformation and elasticity of polymer networks,'' Macromolecules **30**, 8036–8044 (1997).

Viovy, J. L., M. Rubinstein, and R. H. Colby, ''Constraint release in polymer melts: Tube reorganization versus tube dilation,'' Macromolecules **24**, 3587–3596 (1991).

Watanabe, H., Y. Matsumiya, and T. Inoue, ''Dielectric and viscoelastic relaxation of highly entangled star polyisoprene: Quantitative test of tube dilation model,'' Macromolecules **35**, 2339–2357 (2002).

Wischnewski, A., M. Monkenbusch, L. Willner, D. Richter, A. E. Likhtman, T. C. B. McLeish, and B. Farago, ''Molecular observation of contour-length fluctuations limiting topological confinement in polymer melts—Article No. 058301,'' Phys. Rev. Lett. **88**, 058301 (2002).

Ye, X., R. G. Larson, C. Pattamaprom, and T. Sridhar, ''Extensional properties of monodisperse and bidisperse polystyrene solutions,'' J. Rheol. **47**, 443–468 (2003).